

RSC Advances



This is an *Accepted Manuscript*, which has been through the Royal Society of Chemistry peer review process and has been accepted for publication.

Accepted Manuscripts are published online shortly after acceptance, before technical editing, formatting and proof reading. Using this free service, authors can make their results available to the community, in citable form, before we publish the edited article. This *Accepted Manuscript* will be replaced by the edited, formatted and paginated article as soon as this is available.

You can find more information about *Accepted Manuscripts* in the [Information for Authors](#).

Please note that technical editing may introduce minor changes to the text and/or graphics, which may alter content. The journal's standard [Terms & Conditions](#) and the [Ethical guidelines](#) still apply. In no event shall the Royal Society of Chemistry be held responsible for any errors or omissions in this *Accepted Manuscript* or any consequences arising from the use of any information it contains.

Mixed Amido-cyclopentadienyl Group 4 Metal Complexes

Aleš Havlík,^{a,b} Martin Lamač,^a Jiří Pinkas,^a Aleš Růžička,^b and Michal Horáček^{*a}

^a *J. Heyrovský Institute of Physical Chemistry, Academy of Sciences of the Czech Republic, v.v.i., Dolejškova 3, 182 23 Prague 8, Czech Republic*

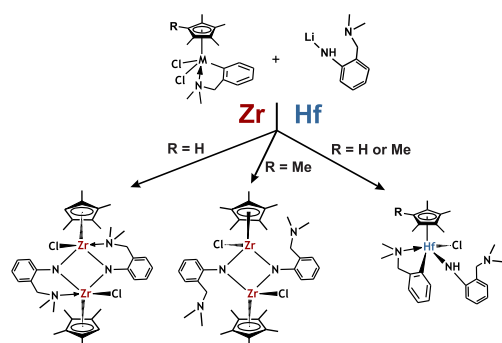
^b *Department of General and Inorganic Chemistry, Faculty of Chemical Technology, University of Pardubice, Studentská 573, 532 10 Pardubice 2, Czech Republic*

* Corresponding author

Phone: (+420) 26605 3965. Fax: (+420) 28658 2307. E-mail addresses: michal.horacek@jh-inst.cas.cz

Table of contents entry

Two different kinds of nitrogen ligands and two Cp ligands with different electronic and steric effects were employed in order to demonstrate variability of the Group 4 metal coordination spheres.



Abstract

The reactivity of substituted half-sandwich complexes of Ti, Zr, and Hf towards 2,6-diisopropylaniline $\text{NH}_2\text{C}_6\text{H}_3-2,6-^i\text{Pr}_2$ ($\text{L}^{\text{N}}\text{H}$) and 2-[(dimethylamino)methyl]aniline $\text{NH}_2\text{C}_6\text{H}_4-2-$

(CH₂NMe₂) (L^{NN}H) was investigated. Two series of mononuclear complexes ($\eta^5\text{-C}_5\text{Me}_5$)L^NMCl₂ (M = Ti (**3**), Zr (**4**), Hf (**5**)) and ($\eta^5\text{-C}_5\text{Me}_5$)L^{NN}MCl₂ (M = Ti (**7**), Zr (**8**), Hf (**9**)) were prepared from corresponding (pentamethylcyclopentadienyl)metal trichlorides and lithium precursors L^NLi and L^{NN}Li. Besides the desired products dimeric hafnium compound [($\eta^5\text{-C}_5\text{Me}_5$) $\{\mu\text{-NC}_6\text{H}_4\text{-2-(CH}_2\text{NMe}_2)\}$ HfCl]₂ (**10**) was also isolated and structurally characterized. The formation of dimeric complexes of this type was also achieved by reacting a series of ($\eta^5\text{-C}_5\text{Me}_4\text{R}$)L^{CN}MCl₂ (M = Zr, Hf; R = Me, H; L^{CN} = C₆H₄-2-(CH₂NMe₂)- $\mu^2\text{C,N}$) complexes with lithium precursors L^NLi and L^{NN}Li generating [($\eta^5\text{-C}_5\text{Me}_4\text{H}$) $\{\mu\text{-NC}_6\text{H}_3\text{-2,6-}^i\text{Pr}_2\}$ MCl]₂ (M = Zr (**11**), Hf (**13**)), [($\eta^5\text{-C}_5\text{Me}_5$) $\{\mu\text{-NC}_6\text{H}_3\text{-2,6-}^i\text{Pr}_2\}$ MCl]₂ (M = Zr (**12**), Hf (**14**)), [($\eta^5\text{-C}_5\text{Me}_4\text{H}$) $\{\mu\text{-NC}_6\text{H}_4\text{-2-(CH}_2\text{NMe}_2\text{)-}\mu^2\text{N,N}\}$ ZrCl]₂ (**15**), and [($\eta^5\text{-C}_5\text{Me}_5$) $\{\mu\text{-NC}_6\text{H}_4\text{-2-(CH}_2\text{NMe}_2)\}$ ZrCl]₂ (**16**), respectively. The formation of **10** by this reaction procedure was not detected; instead monomeric complexes ($\eta^5\text{-C}_5\text{Me}_4\text{R}$)L^{NN}L^{CN}HfCl (R = H (**17**), Me (**18**)) were observed as major products. NMR and IR spectroscopy techniques and elemental analysis were used for characterization of the prepared complexes, whereas the structures in most cases were determined by X-ray crystallography.

Introduction

The significant interest of several research groups in the area of half-sandwich cyclopentadienyl–amino, –amido, and –imido substituted Group 4 compounds is driven mainly by their applications in catalytic transformations of unsaturated compounds.¹ The development of new imido-supported non-metallocene olefin polymerization catalysts seems to be a popular area in the present time.²

Earlier works in the field of early transition metal amide and imide complexes were reviewed by Nugent and Haymore³ and Gade and Mountford.⁴ In the latter article, structures of titanium complexes bearing ligands with adjacent donor functional groups and their reactivity towards unsaturated compounds are described. Mindiola⁵ summarized the work on novel metal-ligand multiply bonded archetypes including the M=NR⁶ one which could be described as a nitrene group (:NR) and which parallels the metal-carbon double bond functionality (carbene :CR₂). The preparation of these complexes is connected to the oxidatively induced α -hydrogen deprotonation of metal-bound amide in low valent titanium

species. Such compounds are acting in various catalytic processes such as hydroamination, hydrohydrazination, aziridination, multicomponent coupling reactions, guanylations, and carboamination. For example, titanium hydrazido and imido complexes containing a pyrrolyl-based ligand are active in hydroamination of alkynes.⁷

Mono- and dinuclear hafnium imido complexes containing bulky Cp* (Cp* = η^5 -pentamethylcyclopentadienyl-) and arylsilyl ligands were prepared by Tilley.⁸ Continuation of work on this topic (for titanium) with simpler and improved synthetic procedures and a plethora of structure descriptions of titanium imides were reported by Lorber.⁹ The homo- and heterobimetallic complexes of Ti, Zr, Hf, V, and Mo with amido and imido ligands in both bridging and terminal positions were isolated recently.¹⁰ In the Ti/Mo heterobimetallic systems the η^6 -arene-coordinated Mo atom can act as a central atom in a Fischer-type carbene.^{10b} Structures of amide-chloride and amide-imide complexes of Group 4 metals containing rather bulky hexamethyldisilazide ligands with cyclic as well as acyclic frameworks were also determined.¹¹

Ligands bearing additional functional groups attached to the amide/imide moiety were also applied. For example, phosphine-substituted anilines were used by Bochmann for the preparation of imido bridged titanium complexes incorporating the central four membered Ti₂N₂ ring. The presence of adjacent phosphine donor groups was further utilized for the complexation of platinum metals. Moreover, the titanium complexes revealed promising activity in the polymerization of ethylene without a change of the central Ti₂N₂ framework upon activation by MAO (Methylaluminoxane).¹² Both amido- and imidoethylpyridine and aniline *N*-bridged titanium complexes with the pendant and potentially chelating *N*-groups ([N(R)(CH₂CH₂py)], py = C₅H₄N, R = SiMe₃, Si^{*t*}BuMe₂, Ph) were described by Martins.¹³

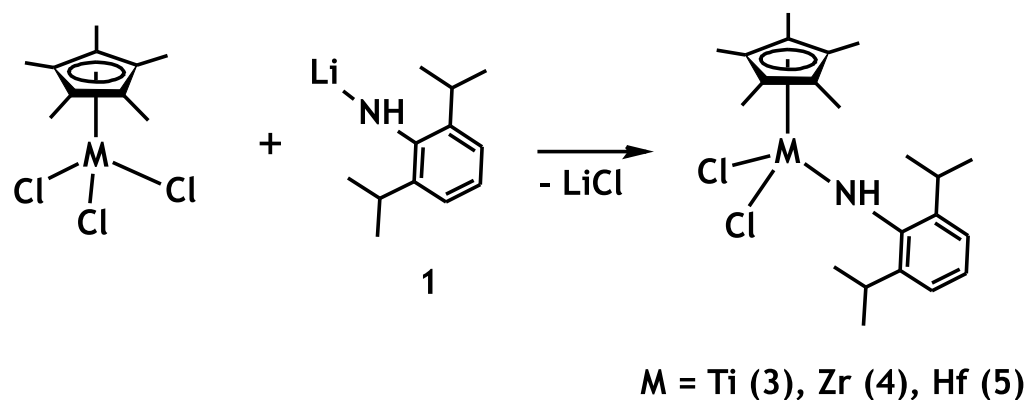
The chemistry of Group 4 amides or imides containing a η^5 -cyclopentadienyl or related ring is rather rich in structural motifs. These motifs are represented by the amide Cp*TiCl₂NH-^{*t*}Bu¹⁴, bis-amides [N(Me)C₆H₃-2,6-^{*i*}Pr₂]₂Cp*ZrCl¹⁵, [(η^5 -1,3-Me₂C₅H₂)Ti(NMe₂)₂Cl]-CH₂-[(η^5 -C₉H₉)Ti(NMe₂)₂Cl],¹⁶ and CpTiCl(NMe₂)₂¹⁷ (Cp = η^5 -cyclopentadienyl-), tris-amides Cp*Zr(NH-^{*t*}Bu)₃ and Cp*Hf(L^N)₃¹⁸, and chelating bis-amides¹⁹. Dinuclear mono- and dicyclopentadienyl complexes with four-membered symmetrical rings formed of two metal atoms bridged usually by two imido nitrogen atoms are the dominant group of complexes in this field.^{8, 18, 20} Other compounds of similar constitution are the products of nitrogen

activation by a low-valent metallocene moiety.²¹ Higher nuclearity or cyclic compounds are also known.^{21i, 21j, 22}

Being interested in the preparation and potential use of bifunctional compounds of mainly Group 4 metals, we described in our previous work a simple method for the preparation of compounds containing a highly substituted cyclopentadienyl ring and the *C,N*-chelating ligand $C_6H_4-2-(CH_2NMe_2)-\mu^2C,N(L^{CN})^{23}$ or bifunctional β -diketiminato ligands with the potentially coordinating methoxy groups²⁴. When we tried to introduce another sterically demanding substituent like 2, 6-diisopropylaniline into the coordination sphere of these metal ions the formation of dimeric compounds with arylimide bridges accompanied by release of *C,N*-chelating ligand were observed. These unexpected results led us to perform a comparative study of such a phenomenon using a sterically demanding as well as *N,N*-chelating anilines.

Results and discussion

The complexes $(\eta^5-C_5Me_5)MCl_3$ ($M = Ti, Zr, Hf$) react smoothly with one equivalent of $L^N Li$ (**1**) to afford complexes $(\eta^5-C_5Me_5)L^N MCl_2$ ($M = Ti$ (**3**), Zr (**4**), Hf (**5**)) and $LiCl$ (Scheme 1).



Scheme 1. Preparation of compounds **3** - **5**

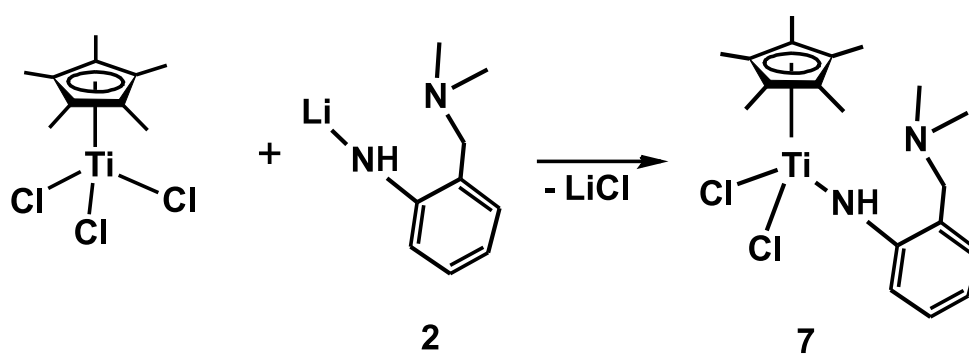
A difference in long-term stability of the prepared amide complexes was observed. Whereas the isolable yield of Zr and Hf complexes was more than 50%, the Ti complex could not be isolated sufficiently pure in larger amount due to its decomposition. NMR spectra of

the crude product were, however, in line with the proposed structure, notably displaying a signal due to the N-H hydrogen at δ 9.51 ppm. Moreover, we were able to isolate several crystals of **3** suitable for X-ray analysis directly from the cooled reaction mixture. The molecular structure of **3** obtained by X-ray analysis showed that the expected product was formed. Nevertheless, further processing of the crude product led to the formation of a mixture of yet unidentified compounds which do not contain N-H bond (according to NMR and IR spectroscopy). This could be due to the thermolytic α -hydrogen abstraction from the metal-bound amide by a chlorine atom as described by Tilley for hafnium complexes.⁸

In contrast, zirconium and hafnium complexes **4** and **5** are stable and were isolated and characterized by NMR and IR spectroscopy. ¹H and ¹³C NMR spectra of amide complexes **4** and **5** supported the proposed structures. The signal of the amine hydrogen is downfield shifted (6.37 ppm for **4** and 6.02 for **5**) in comparison to the free 2,6-diisopropylaniline ligand ($\delta_{\text{H}} \text{NH (TOL-D}_8\text{)}$: 3.18 ppm). Infrared spectra of **4** and **5** complexes displayed absorption bands corresponding to N-H stretching vibration at 3352 cm⁻¹ for **4** and 3355 cm⁻¹ for **5**. There are also present the aromatic C-H stretching vibration at 3062 cm⁻¹ and strong absorption for C-H out of plane deformation bands at 750 cm⁻¹ typical for an ortho-substituted benzene ligand. The asymmetric stretching vibration of methyl groups in Cp* ligands were observed at 2962-2869 cm⁻¹, and their asymmetric deformation vibration in range 1460-1430 cm⁻¹. The strong deformation vibration corresponding to methyl groups in 2,6-diisopropylaniline ligand were found at 1380 cm⁻¹.

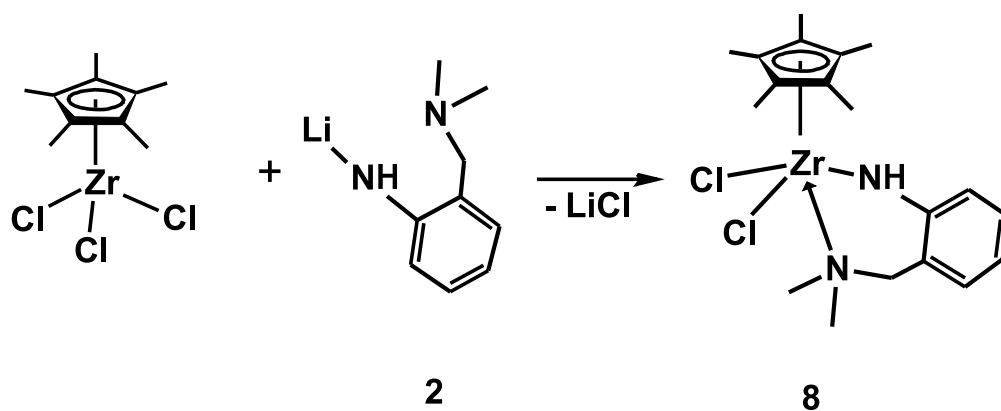
In addition, minor product ($\eta^5\text{-C}_5\text{Me}_5$)L^{NN}₃Zr (**6**) was obtained from crude reaction mixture of zirconium containing species in a form of several colourless crystals. The molecular structure of this compound was determined by X-ray crystallography and revealed the presence of three L^{NN} ligands in this complex (see Figure 4). Similar structures are known from literature for -NHR R = ^tBu; 2,4,6-Me₃C₆H₂ and 2,6-ⁱPr₂C₆H₃ ligands.¹⁸

In order to increase the stability of titanium compound **3** reactions of ($\eta^5\text{-C}_5\text{Me}_5$)MCl₃ (M = Ti, Zr, Hf) with L^{NN}Li (**2**) were carried out. This ligand contains in addition to the NH group a lone electron pair on the tethered NMe₂ group. The results show a different behaviour of the elements of Group 4, which reflects their different capability of adopting higher coordination numbers. Thus, the titanium complex reacted with **2** under elimination of LiCl and afforded the complex ($\eta^5\text{-C}_5\text{Me}_5$)L^{NN}TiCl₂ (**7**), where the dimethylamino group of the ligand is not involved into the bonding to the titanium centre (Scheme 2).



Scheme 2. Synthesis of compound **7**.

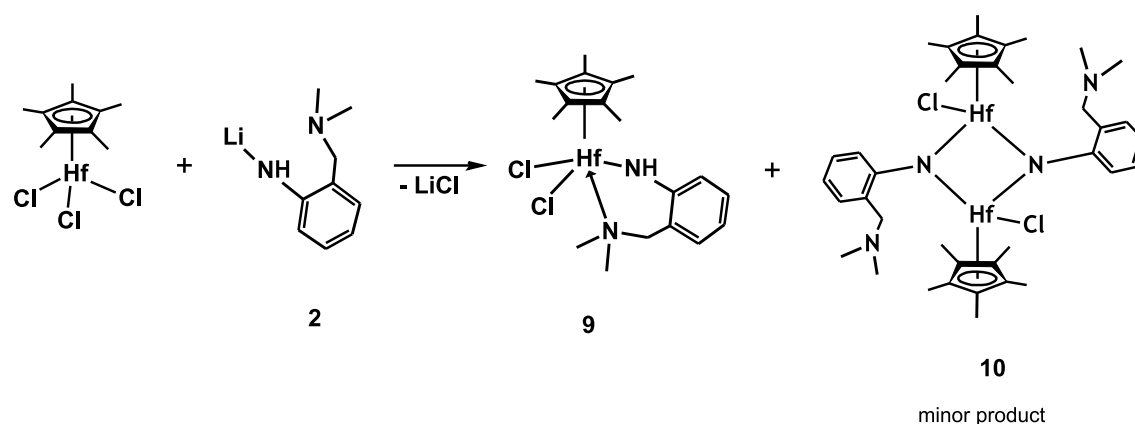
On the other hand zirconium and hafnium major products ($\eta^5\text{-C}_5\text{Me}_5\text{L}^{\text{NN}}\text{MCl}_2$ (M = Zr(**8**), Hf(**9**))) are stabilized via the intramolecular coordination of NMe₂ group of the ligand. Half-sandwich zirconium trichloride reacts with one equivalent of **2** to form monomeric complex **8** in a high yield (Scheme 3).



Scheme 3. Synthesis of compound **8**.

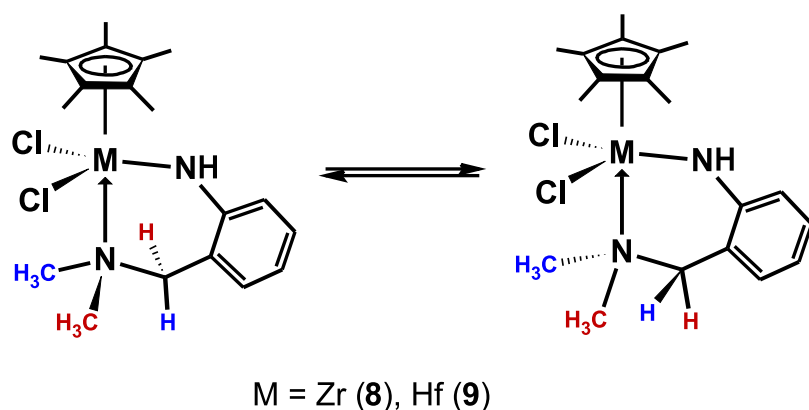
Half-sandwich hafnium trichloride reacts with one equivalent of **2** in a similar way as the zirconium compound. As a minor product of this reaction several single-crystals of complex **10** were isolated from the crude mixture. The X-ray measurement determined the molecular structure of this product as the dimeric complex $[(\eta^5\text{-C}_5\text{Me}_5)\{\mu\text{-NC}_6\text{H}_4(\text{CH}_2(\text{NMe}_2))\}]\text{HfCl}_2$ (**10**), where two nitrogen atoms act as bridges between two hafnium atoms (Scheme 4).

Formation of this compound is a consequence of the α -H abstraction from the L^{NN} ligand by chloride atom with the assistance of a base, probably free $L^{NN}H$ molecule.



Scheme 4. Synthesis of compound **9**.

Solutions of complexes **8** and **9** in toluene- D_8 exhibited a fluxional behaviour in the studied range of temperatures (228-328 K) as observed by NMR spectroscopy (see Supporting Information). At lower temperature the complexes possessed an unsymmetrical structure with the dimethylamino group coordinated to the metal centre (similarly as was proved in the solid state) which is in accordance with the presence of two singlets for non-equivalent methyl groups (2.17, 2.72 ppm for **8** and 2.15, 2.66 ppm for **9**) and a system of two doublets for diastereotopic methylene hydrogens (2.51, 5.00 ppm, $^2J_{HH} = 13.3$ Hz for **8** and 2.47, 4.93 ppm, $^2J_{HH} = 13.3$ Hz for **9**) in 1H NMR spectra. Upon heating, the signals became broader, coalesced and finally only an average signal could be observed as a consequence of fast interconversion between the pair of enantiomers (see Scheme 5).



Scheme 5. Dynamic behaviour of compounds **8** and **9** observed by NMR

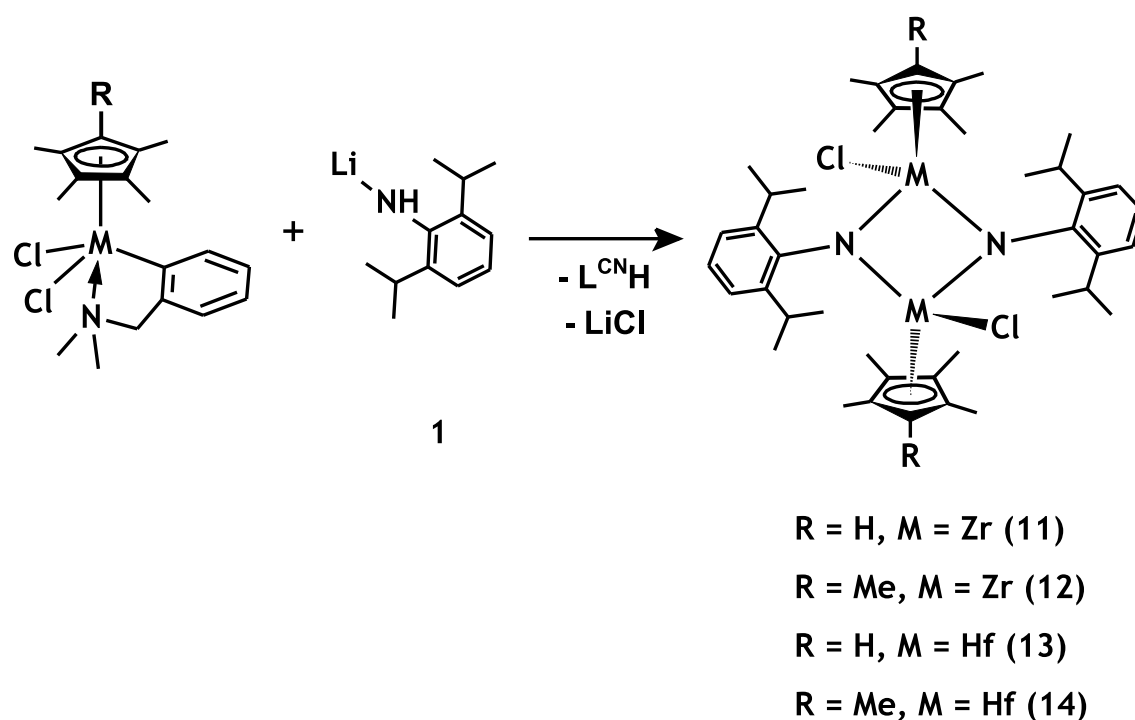
The line-shape analysis with the WINDNMR program²⁵ of spectra taken at different temperatures allowed us to determine the corresponding thermodynamic parameters ($\Delta H^\ddagger = 45.8 \pm 1.4 \text{ kJ}\cdot\text{mol}^{-1}$, $\Delta S^\ddagger = -24.3 \pm 5.0 \text{ J}\cdot\text{K}^{-1}\cdot\text{mol}^{-1}$, $\Delta G^\ddagger_{298} = 53.1 \text{ kJ}\cdot\text{mol}^{-1}$ for **8**; $\Delta H^\ddagger = 39.0 \pm 1.2 \text{ kJ}\cdot\text{mol}^{-1}$, $\Delta S^\ddagger = -37.4 \pm 4.5 \text{ J}\cdot\text{K}^{-1}\cdot\text{mol}^{-1}$, $\Delta G^\ddagger_{298} = 50.2 \text{ kJ}\cdot\text{mol}^{-1}$ for **9**) from the respective Eyring plots (see Supporting Information). The obtained ΔG^\ddagger values are lower in comparison to the corresponding L^{CN} complexes ($\Delta G^\ddagger_{298} = 57.8 \text{ kJ}\cdot\text{mol}^{-1}$ for $\text{Me}_5\text{ZrL}^{\text{CN}}$ and $\Delta G^\ddagger_{298} = 64.6 \text{ kJ}\cdot\text{mol}^{-1}$ for $\text{Me}_5\text{HfL}^{\text{CN}}$).²³ We suggest that two phenomena contribute to the decrease of rotation barrier in L^{NN} complexes. The higher electronic saturation of the metal with amide group (from L^{NN} ligand) in comparison to aryl group (from L^{CN} ligand) decrease the Lewis acidity of the metal and consequently weaken the coordination of the dimethylamine functionality as could be demonstrated with lower ΔH^\ddagger values in L^{NN} when compared to L^{CN} ($\Delta H^\ddagger = 77.4 \pm 1.9 \text{ kJ}\cdot\text{mol}^{-1}$ for $\text{Me}_5\text{ZrL}^{\text{CN}}$ and $\Delta H^\ddagger = 66.9 \pm 2.6 \text{ kJ}\cdot\text{mol}^{-1}$ for $\text{Me}_5\text{HfL}^{\text{CN}}$).²³ Furthermore, the formation of six-membered metal-amido-amino ring in L^{NN} complexes (only 5-membered ring is constituted in L^{CN} complexes) pushes the bulky aryl group away from the metal centre, which also facilitates its rotation leading to faster conformational exchange.

Infrared spectra of **8** and **9** complexes displayed similar absorption bands as previously described for compounds **4** and **5**. Furthermore, stretching C-N vibrations were found for **8** and **9** in the range $1281\text{-}1246 \text{ cm}^{-1}$.

Reactivity of L^{CN} complexes towards lithium amides

Based on a successful Tinkertoy story by Lang²⁶ who prepared multiheterometallic complexes, we followed a reverse approach performing thus reactions leading to the Group 4 complexes containing four different ligands, which could be interesting from the point of view of mutual comparison of coordination abilities of selected donors and last but not least suggested formation of a stereogenic centre. Recently we reported the synthesis of Group 4 metal complexes containing a pentamethyl- or tetramethyl-substituted cyclopentadienyl ring and C,N-chelating ligand L^{CN}.²³ In order to prepare new compounds containing four different ligands in coordination sphere of Group 4 metals we have tested the reaction of zirconium and hafnium complexes of this type with lithium salts of **1** and **2**. Titanium containing complexes were omitted due to lower stability of the corresponding amido compounds.

$(\eta^5\text{-C}_5\text{Me}_4\text{R})\text{L}^{\text{CN}}\text{MCl}_2$ (M = Zr, Hf; R = Me, H) complexes react under mild conditions with **1** to eliminate LiCl together with L^{CN} ligand and generate the dimeric products $[(\eta^5\text{-C}_5\text{Me}_4\text{H})\{\mu\text{-NC}_6\text{H}_3\text{-2,6-}^i\text{Pr}_2\}\text{MCl}]_2$ (M = Zr (**11**), Hf (**13**)) and $[(\eta^5\text{-C}_5\text{Me}_5)\{\mu\text{-NC}_6\text{H}_3\text{-2,6-}^i\text{Pr}_2\}\text{MCl}]_2$ (M = Zr (**12**), Hf (**14**)) (Scheme 6). The likely intermediate containing bonded L^N ligand is arising after transmetalation reaction and elimination of LiCl. In the next step the presence of amino group with reactive hydrogen atom in the neighbourhood of L^{CN} ligand leads to the α -hydrogen abstraction and elimination of L^{CN}H molecule. Finally the dimeric structure is formed. The driving force for the dimer formation is in this case the increase of electron density at the electron deficient central metal atom. Solid state structures of complexes **11** - **14** were determined by X-ray crystallography and the molecular structures were confirmed by NMR spectroscopy also in solutions. Both dimers have similar molecular structure as complex **10** obtained earlier as a minor side product as depicted in Scheme 4. Hafnium complex **14** was previously prepared by Tilley et al. by thermolysis of hafnium silyl complex $\text{Cp}^*\text{Hf}[\text{Si}(\text{SiMe}_3)_3]\text{L}^{\text{N}}\text{Cl}$.⁸



Scheme 6. Preparation of compounds **11** - **14**.

^1H and ^{13}C NMR spectra of solutions of complexes **11**, **12**, **13**, and previously published **14** differed from the above mentioned amide complexes **4** and **5**. Apart from the missing NH signal, the most significant feature is the presence of two sets of doublets (centred at: 1.22 and 1.47 ppm in **12**; 1.31 and 1.39 ppm in **11**, 1.29, 1.51 ppm in **14**,⁸ 1.26 and 1.42 ppm in **13**) for non-equivalent methyl groups of iso-propyl moiety. The spectral pattern is consistent with bridging imido moieties between two metal atoms, showing that the solid state structure (found by X-ray) is retained in the solution. Upfield shift of C_5Me_5 signal in ^1H NMR spectra of imido complexes ($\delta_{\text{H}} \text{C}_5\text{Me}_5$: 1.76 ppm in **12**; 1.83 ppm in **14**) in comparison to amide complexes **4** ($\delta_{\text{H}} \text{C}_5\text{Me}_5$: 1.88 ppm) and **5** ($\delta_{\text{H}} \text{C}_5\text{Me}_5$: 1.92 ppm) reflects higher electron saturation of the metal centre with two bridging imido ligands in comparison to chloride ligand.

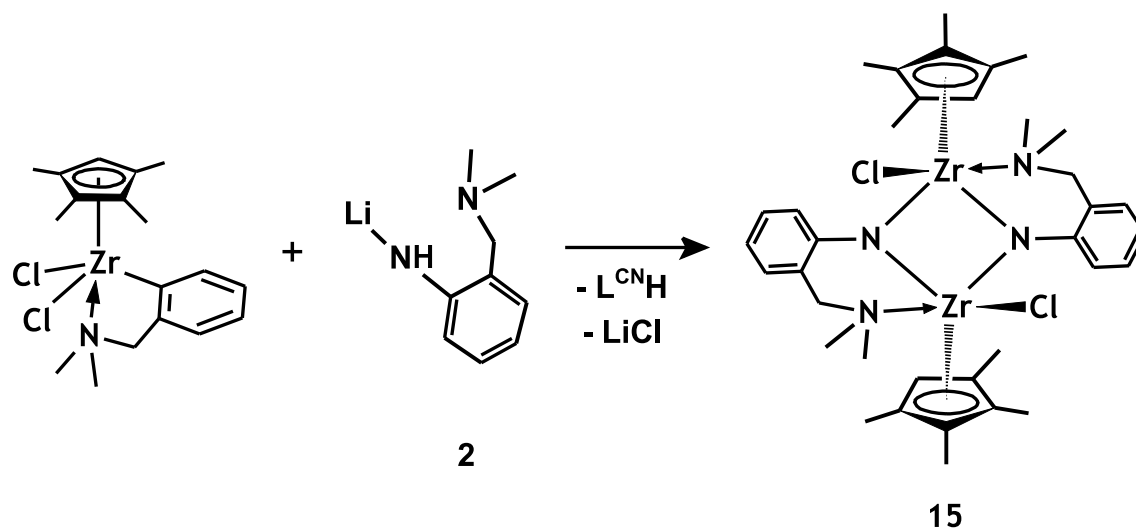
Infrared spectra of these dimers **11** - **13** display aromatic C-H stretching vibration 3052 cm^{-1} and strong absorption for C-H out of plane deformation bands at 750 cm^{-1} typical for ortho-substituted benzene ligand. The asymmetric stretching vibration of methyl groups in Cp^* and Cp' ligands were observed at $2981\text{-}2869\text{ cm}^{-1}$ and the strong absorption band belonging to stretching C-N vibration was found at 1169 cm^{-1} .

The results from the study of reactivity of L^{CN} complexes with compound **1** encouraged us perform the same reactions with compound **2**, too. We expected the formation of dimeric compounds with a bridging imide derived from the L^{NN} ligand. Moreover the formation of the by-product **10** in previously mentioned reaction proved that such complexes can be obtainable.

The expectations were fulfilled only partially, results show differences in the behaviour of zirconium and hafnium derivatives, with a significant role of substitution on the cyclopentadienyl ring having an influence on the structure of the products.

Zirconium complexes containing permethylated and tetramethylated cyclopentadienyl ring ($\eta^5\text{-C}_5\text{Me}_4\text{R}$) $L^{CN}\text{ZrCl}_2$ ($R = \text{H, Me}$) were reacted with **2** under the same conditions as half-sandwich zirconium trichlorides (Scheme 7 and 8). The main products of the reactions were isolated as orange crystals suitable for X-ray analysis. Reaction mixtures as well as isolated crystals were studied by NMR and IR spectroscopy. In both cases, elimination of LiCl as a white precipitate and the liberated ligand (L^{CNH}) was observed by NMR spectroscopy. The products are dimeric zirconium μ -imido complexes containing besides the bridging ligands two substituted cyclopentadienyl rings and two chlorine atoms $[(\eta^5\text{-C}_5\text{Me}_4\text{H})\{\mu\text{-NC}_6\text{H}_4\text{-2-(CH}_2\text{NMe}_2)\}\mu^2\text{N,N}\text{ZrCl}]_2$ (**15**) and $[(\eta^5\text{-C}_5\text{Me}_5)\{\mu\text{-NC}_6\text{H}_4\text{-2-(CH}_2\text{NMe}_2)\}\text{ZrCl}]_2$ (**16**).

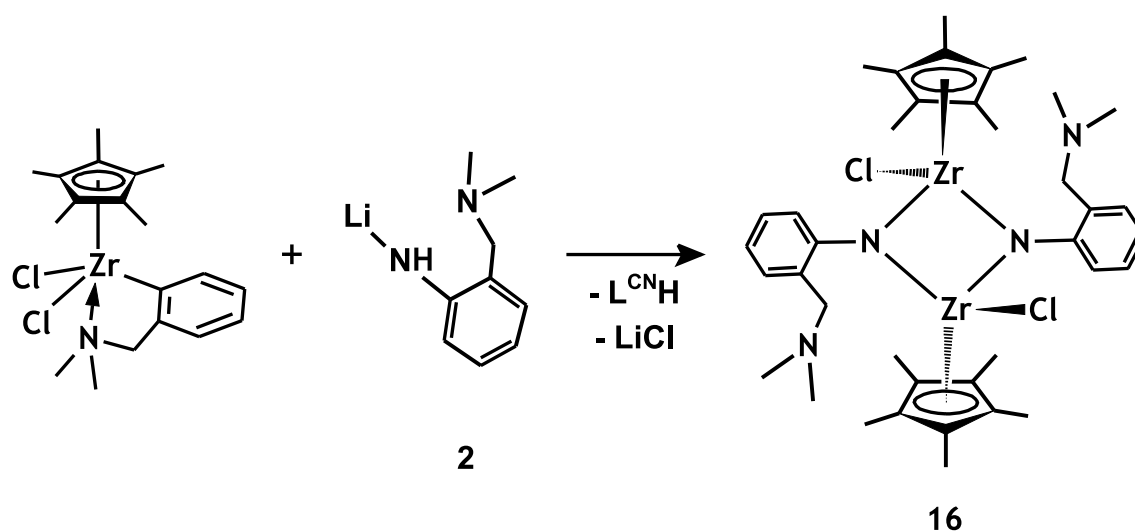
While the tetramethylcyclopentadienyl-containing counterpart **15** shows a structure where pendant (dimethylamino)methyl arms are coordinated to the metal centres, the same N-donor groups in its Cp*-containing dimer **16** are uncoordinated to zirconium atoms.



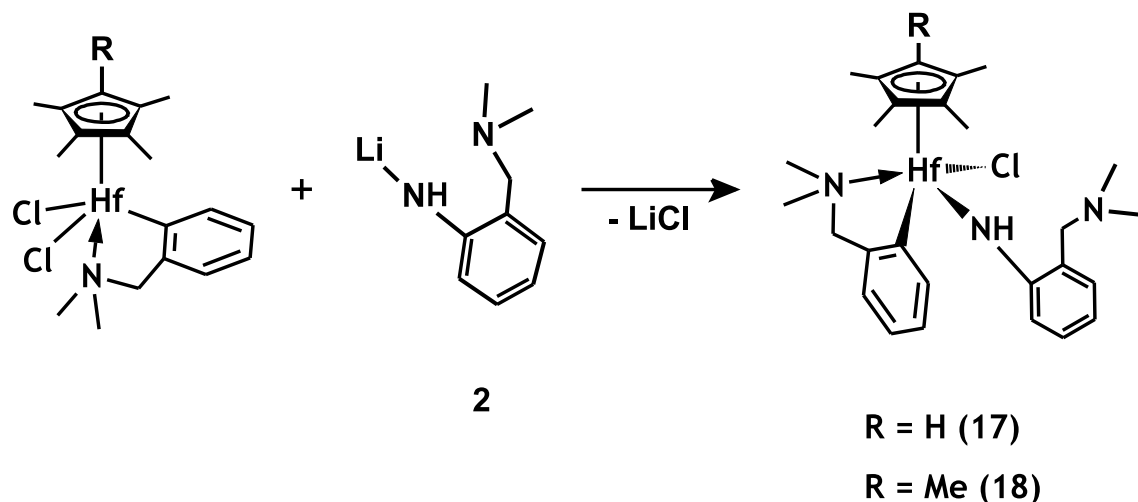
Scheme 7. Synthesis of compound **15**.

NMR spectra of dimer **15** are consistent with the structure confirmed by X-ray diffraction (vide infra), which gives rise to one set of signals (syn- isomer) due to the C_5Me_4H and imide ligands. Coordinated pendant amine arms are likely undergoing dynamic conformational changes as evidenced by broad singlet signals for NMe_2 groups. On the contrary, compound **16** was likely obtained as a mixture of syn-/anti- isomers from which only the crystals of the anti-isomer were analysed by X-ray diffraction (vide infra). NMR spectroscopy of the bulk crystalline product, however, reveals two sets of signals corresponding to both isomers. Both of them have the same spectral pattern with doublet signals due to diastereotopic methylene hydrogens of the L^{NN} ligand, however, in comparison to **15** the difference in chemical shifts between these two signals is smaller and, furthermore, signals of NMe_2 groups appear as sharp singlets. This all suggests that the (dimethylamino)methyl arms in both isomers of **16** remain uncoordinated in solution as well as in the solid state, which is probably caused by an increased steric bulkiness of the C_5Me_5 ligand.

Infrared spectra of complexes **15** and **16** displayed similar absorption bands as previously described for compounds **8** and **9** except the N-H stretching vibration which is missing.

Scheme 8. Synthesis of compound **16**.

In line with generally lower reactivity of Hf complexes ($(\eta^5\text{-C}_5\text{Me}_4\text{R})\text{L}^{\text{NN}}\text{L}^{\text{CN}}\text{HfCl}$ (R = H (**17**), Me (**18**)) were obtained from the reactions of complexes $(\eta^5\text{-C}_5\text{Me}_4\text{R})\text{L}^{\text{CN}}\text{HfCl}_2$ (R = Me, H) with **2** (Scheme 9). Both compounds were formed by a substitution of one chloride ligand with the corresponding L^{NN} amide, while the L^{CN} ligand remained unaffected. NMR spectra of both **17** and **18** showed the presence of both ligands as distinguishable sets of signals. The L^{NN} amides gave rise to a characteristic NH signal in ^1H spectra at δ 8.71 ppm for **17** or 8.46 ppm for **18**, respectively. The presence of the NH group was confirmed by infrared spectra that show N-H stretching vibration at 3276 cm^{-1} for **17** and 3235 cm^{-1} for **18**, respectively. The structure and stability of these monomeric hafnium complexes shows that the reaction pathway leading to formation of zirconium and hafnium dimers goes through such species. We can assume that the intermediate in the formation of dimeric complexes should be the same; however, in the case of zirconium being more prone to α -hydrogen abstraction than in the hafnium one.



Scheme 9. Preparation of compounds **17** and **18**.

Solid state study

Structures of **3** - **5** are the only crystallographically determined structures in the series reported in this paper, where the combination of one substituted Cp and one 2,6-(diisopropyl)phenylanilide (L^{N}) is present in a mononuclear complex (for molecular structure of **5** see Figure 1, for molecular structures of **3** and **4** see Supporting Information). Structures

of **3** - **5** can be compared to the only example of such kind of compounds, containing both amide and Cp ligands - $\text{Cp}^*\text{TiCl}_2\text{NH-}^t\text{Bu}^{14}$, from the point of view of the structural arrangement, but the direct comparison of bond lengths and angles is possible only with **3**, because of covalent radii differences between Ti and Zr/Hf atoms ($\sim 0.15 \text{ \AA}$). The ring centroid to the titanium atom distance is slightly ($\sim 0.01 \text{ \AA}$) longer in $\text{Cp}^*\text{TiCl}_2\text{NH-}^t\text{Bu}^{14}$ than in **3**, but a shortening of similar magnitude is found for the rest of the distances in the titanium atom vicinity. Mutual comparison of **3** - **5** reveals close structures with an elongation of metal-ligand distances for higher congeners of titanium only. On the other hand, a parallel between **5** and $\text{Cp}^*\text{Hf}(\text{L}^{\text{N}})_3^{18}$ can be drawn, the Hf–Cg(Cp*) and all Hf–N are slightly elongated by ca. 0.06 \AA in $\text{Cp}^*\text{Hf}(\text{L}^{\text{N}})_3$. The same trend can be observed in the case of angles Cg–Hf–N and C–N–Hf which are in $\text{Cp}^*\text{Hf}(\text{L}^{\text{N}})_3$ more opened by ca. 5 and 20° , respectively, probably because of high steric repulsion of three anilide ligands.

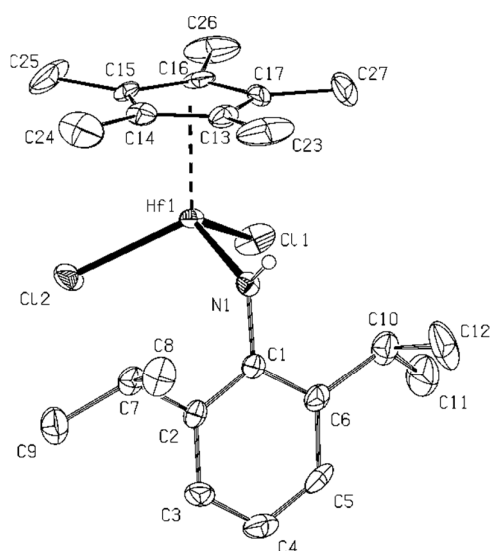


Figure 1. Molecular structure of **5** (ORTEP view, 30% probability level). Hydrogen atoms are omitted (except of H1) for clarity. Selected interatomic distances [\AA] and angles [$^\circ$]: Hf1–N1 2.003(4), Hf1–Cl1 2.3699(17), Hf1–Cl2 2.3680(16), Hf1–Cg1 2.144(3); Cg1–Hf1–Cl1 113.2(4), Cg1–Hf1–Cl2 115.9(3), Cg1–Hf1–N1 111.5(3), C1–N1–Hf1 121.4(3).

In the series where the combination of one substituted Cp and one potentially chelating ligand 2-(dimethylaminomethyl) anilide (L^{NN}) are present, two rather different structures were determined by X-ray diffraction techniques. The first one containing

titanium **7** (Figure 2) is very close to the classical piano stool structure of $\text{Cp}^*\text{TiCl}_2\text{NH-}^t\text{Bu}^{14a}$ with only Ti–N bond slightly elongated due to the presence of N–H...N intramolecular connection. N3 atom of the flexible, potentially chelating arm is out of the primary coordination sphere of the titanium atom as well as from the parent phenyl ring ($55.5(4)^\circ$).

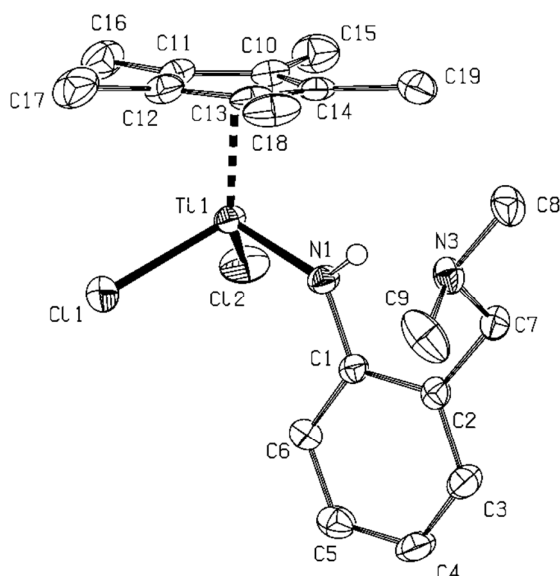


Figure 2. Molecular structure of **7** (ORTEP view, 50% probability level). Hydrogen atoms (except of H1) and the second independent molecule are omitted for clarity. Selected interatomic distances [Å] and angles [°] (appropriate parameters for the second independent molecule are given in parenthesis): Ti1–N1 1.906(3) (1.912(2)), Ti1–N3 4.691(3) (4.637(3)), Ti1–C2 2.2775(10) (2.2783(10)), Ti1–Cl2 2.2648(10) (2.2601(10)), Ti–Cg 2.041(3) (2.028(3)), N1–H1...N3 2.978(4) (2.922(3)); Cg–Ti1–Cl1 118.1(3) (117.4(3)), Cg–Ti1–Cl2 116.7(4) (115.5(3)), Cg–Ti1–N1 110.1(3) (110.7(3)), C1–N1–Ti1 130.7(2) (130.0(2)), C3–C2–C7–N3 55.5(4).

In the structure of the second representative **8** (Figure 3. structures of two geometrically similar solvato-polymorphs of **8** (**8** and **8'**) were determined), this arm is closely interacting with the zirconium center forming nearly perfect trigonal bipyramid. One can estimate, this particular interaction is stronger than the suggested hydrogen bond between two nitrogen atoms found in **7**. The axial positions are occupied by the coordinated nitrogen atom N2 and the centroid of the Cp* ring, while the Zr1–N2 distance of 2.513(3)Å is in the range of the medium strong interactions of these atoms taking into the account the

sum of covalent and van der Waals radii of both atoms.²⁷ Similar distances were also found for interactions of the same type of atoms in complexes of Cp-substituted zirconium complexes bearing related *C,N*-chelating ligand where the coordination polyhedra of the zirconium atom is being tetragonal pyramid.^{23, 28} The equatorial plane is a bit distorted towards the N2 atom, when a plane is defined by two chlorine and nitrogen N1 atoms, the Zr1 atom is 0.509Å above this plane which is nearly parallel to the plane of Cp* ring.

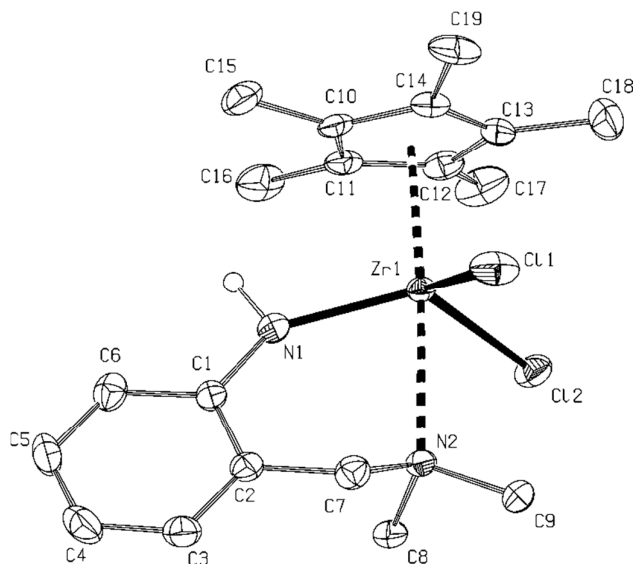


Figure 3. Molecular structure of **8** toluene (ORTEP view, 40% probability level). Hydrogen atoms (except of H1) and toluene solvent molecule are omitted for clarity. Selected interatomic distances [Å] and angles [°]: Zr1–N1 2.093(3), Zr1–N2 2.513(3), Zr1–Cl1 2.4310(10), Zr1–Cl2 2.4511(10), Zr1–Cg1 2.245(4); Cg1–Zr1–Cl1 104.5(3), Cg1–Zr1–Cl2 103.1(2), Cg1–Zr1–N1 100.9(3), Cg1–Zr1–N2 175.2(3), C1–N1–Zr1 140.8(3), C3–C2–C7–41.8(3).

Structure of **6** (Figure 4), as a minor byproduct isolated from preparation of **4** is closely related to the reported structures of Cp*Zr(NH-*t*Bu)₃ and Cp*Hf(L^N)₃, respectively.¹⁸ High steric repulsion of three L^N substituted ligands in comparison to ligands with *t*-Bu substituents in Cp*Zr(NH-*t*Bu)₃ is obviously a reason for different arrangement of ligands in all these three compounds (a *syn* for *t*Bu and an alternate orientation of amido ligands in L^N substituted complexes). In a comparison of relevant geometrical parameters of **6**, to

appropriate ones of **4** and **8**, slightly longer distances in the primary coordination sphere of zirconium atom were observed.

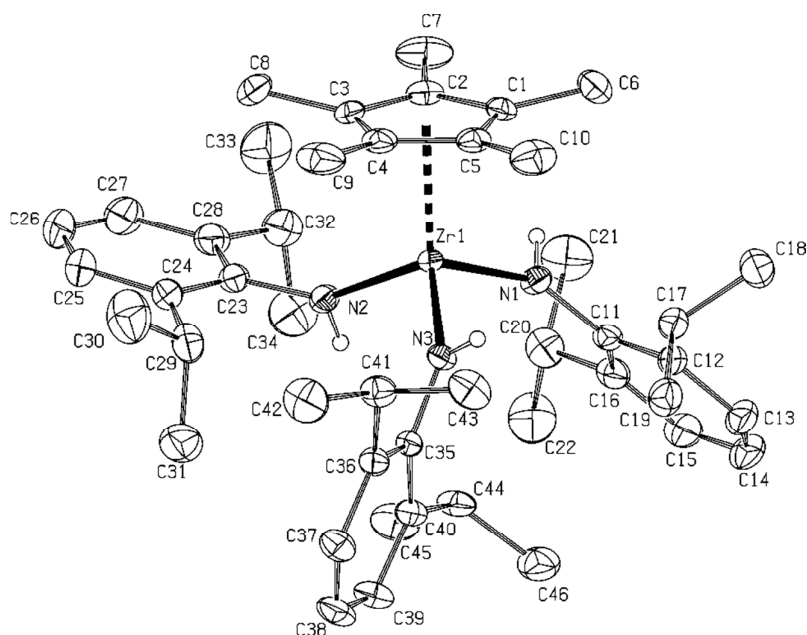


Figure 4. Molecular structure of **6** (ORTEP view, 30% probability level). Hydrogen atoms are omitted (except of H1, H2 and H3) for clarity. Selected interatomic distances [Å] and angles [°]: Zr1–N1 2.0740(16), Zr1–N2 2.0642(16), Zr1–N3 2.0760(15), Zr1–Cg1 2.255(4); Cg1–Zr1–N1 111.45(3), Cg1–Zr1–N2 115.18(3), Cg1–Zr1–N3 115.30(3).

Seven structures of dimers (dinuclear complexes) were determined. All four combinations of Zr, Hf, Cp' and Cp* 2,6-(diisopropyl)phenyl- substituted imido ligand complexes **11** - **14** are from a structural point of view closely related, having central binuclear character, bridged by two imides, with nearly square planar M₂N₂ ring structures and M–N bonds being only slightly unequal. The shape of the metals' coordination polyhedra is pseudotetrahedral. The parallel orientation of the same type of ligand rings, both Cp and phenyls, and metal-chlorine atom bonds with an *anti*-orientation with respect to the plane or the central M₂N₂ motif, is the general phenomenon observed in all these structures. In zirconium **11** (Figure 5) and **12** (Figure 6) as well as in hafnium **13** (Figure 7) and **14** (for molecular structure see Supporting Information Figure S3) compounds, the interatomic distances are slightly longer for Cp* substituted complex probably due to higher sterical

hindrance and electron density of this substituent. The metal-metal distances being around 3.05 Å in all complexes.

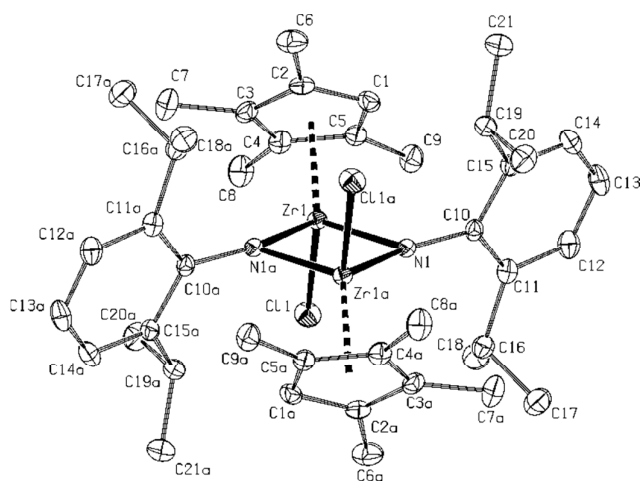


Figure 5. Molecular structure of **11** (ORTEP view, 50% probability level, Symmetry code: (a) $-x, -y+1, -z+1$). Hydrogen atoms are omitted for clarity. Selected interatomic distances [Å] and angles [°]: Zr1–N1 2.1530(16), Zr1–N1a 2.0277(16), Zr1–Cl1 2.4153(5), Zr1–Cg1 2.219(3); Zr1–Zr1a 3.064(4); Cg1–Zr1–Cl1 108.18(3), Cg1–Zr1–N1 122.69(3), Cg1–Zr1–N1a 124.05(2), Cg–Zr1–Zr1a 138.59(3), N1–Zr1–N1a 85.78(6), N1–Zr1–Cl1 106.25(4), N1a–Zr1–Cl1 107.22(5), Zr1–N1–Zr1a 94.22(6), C10–N1–Zr1 111.79(11), C10–N1–Zr1a 153.06(13).

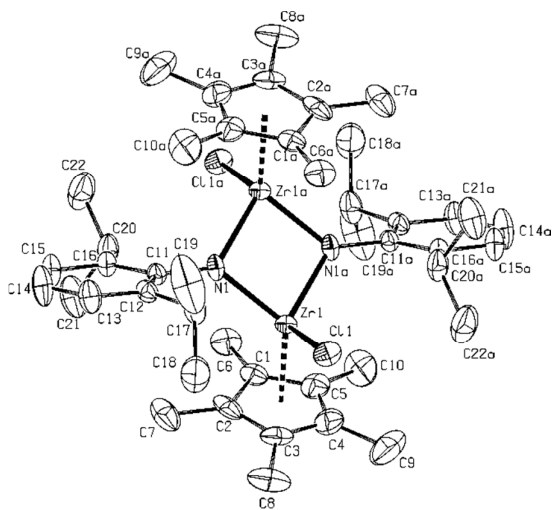


Figure 6. Molecular structure of **12** (ORTEP view, 30% probability level, Symmetry code: (a) $-x+1/2, -y+1/2, -z+1$). Hydrogen atoms are omitted for clarity. Selected interatomic

distances [Å] and angles [°]: Zr1–N1 2.086(4), Zr1–N1a 2.106(4), Zr1–Cl1 2.4280(14), Zr1–Cg1 2.234(3); Zr1–Zr1a 3.092(4); Cg1–Zr1–Cl1 106.42(3), Cg1–Zr1–N1 122.69(2), Cg1–Zr1–N1a 123.79(3), Cg–Zr1–Zr1a 138.00(3), N1–Zr1–N1a 84.96(14), N1–Zr1–Cl1 109.17(11), N1a–Zr1–107.94(11), Zr1–N1–Zr1a 95.05(14), C11–N1–Zr1 135.5(3), C11–N1–Zr1a 129.5(3).

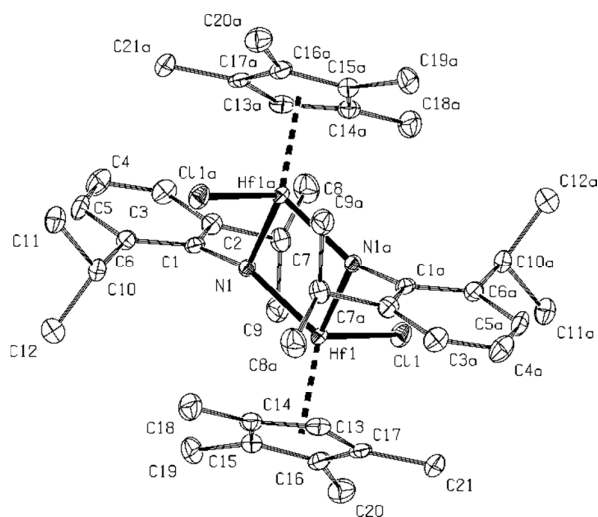


Figure 7. Molecular structure **13** (ORTEP view, 50% probability level, Symmetry code: (a) $-x+1, -y, -z+1$). Hydrogen atoms are omitted for clarity. Selected interatomic distances [Å] and angles [°]: Hf1–N1 2.026(3), Hf1–N1a 2.115(3), Hf1–Cl1 2.3918(9), Hf1–Cg1 2.193(4), Hf1–Hf1a 3.0373(3), N1–Hf1–N1a 85.65(11), N1–Hf1–Cl1 107.14(8), N1a–Hf1–Cl1 105.14(8), Cl1–Hf1–Cg1 108.64(9), N1–Hf1–Cg1 125.23(8), N1a–Hf1–Cg1 122.00(9), N1–Hf1–Hf1a 43.97(8), N1a–Hf1–Hf1a 41.68(8), C16–Hf1–Hf1a 164.22(9).

The structure of the analogue of **11** - **13**, compound **14**, has been determined earlier by Tilley⁸, but the dataset quality did not allowed an anisotropic refinement of lighter atoms. We re-determined the structure in order to have the exact comparison in hands. Again, the hafnium complexes **13** and **14** have slightly shorter metal to other element distances than the zirconium compounds **11** and **12** because of different covalent radii of both atoms while the values of relevant interatomic angles for **11** - **14** are comparable.

Another three structures of complexes **10**, **15** and **16** bearing the potentially *N,N*-chelating ligand were determined. Mutual discrepancy in Hf–N bond lengths within the Hf₂N₂ core of **10** (Figure 8) is a bit larger than in previous cases of **11** - **14**, probably because

of lower bulkiness of the imido ligand but the rest of the parameters is quite similar. In this respect, the Cp* zirconium complex **16** (Figure 9) reveals close structures to **11** - **14** and **10** with the same arrangement and mutual orientation of the ligands. On the other hand, the zirconium-zirconium distance in **16** is elongated by ~ 0.06 Å in comparison to the rest of discussed dinuclear complexes. In this respect, the structure of complex **15** (Figure 10), bearing the chelating L^{NN} and Cp' ligands is also dinuclear but the orientation of Cp rings and chloro ligands is mutually syn. The aromatic rings are perpendicularly oriented with pendant amino groups being as strongly coordinated to the zirconium atoms as in the case of **4**. The Zr–Cl and Zr–Cg1, and more significantly in the Zr1–Zr1a case, these distances are longer than in the rest of dinuclear cases, because of an increase of electron density on the zirconium atoms, and also by the change of the pseudotetrahedral metal neighborhood to the square pyramidal one.

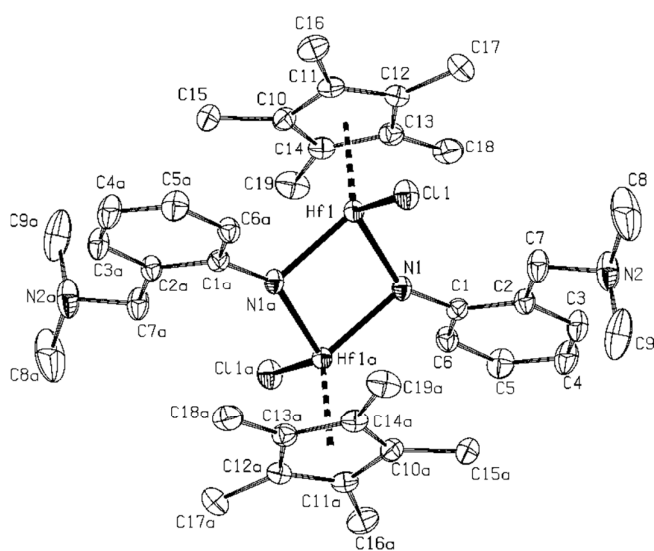


Figure 8. Molecular structure of **10** (ORTEP view, 50% probability level, Symmetry code: (a) $-x, -y, -z+2$). Hydrogen atoms are omitted for clarity. Selected interatomic distances [Å] and angles [°]: Hf1–N1 2.012(3), Hf1–N1a 2.106(3), Hf1–Cl1 2.4090(8), Hf–N2 5.172(3), Hf1–Cg1 2.174(3); Cg1–Hf1–Cl1 111.74(3), Hf1–Hf1a 3.068(4), Cg1–Hf1–N1 117.55(3), Cg1–Hf1–N1a 123.55(3), Cg1–Hf1–Hf1a 133.06(3), N1–Hf1–N1a 83.71(11), N1–Hf1–Cl1 107.63(8), N1a–Hf1–Cl1 109.13(8), Hf1–N1–Hf1a 96.29(11), C1–N1–Hf1 147.4(2), C1–N1–Hf1a 115.6(2), C3–C2–C7–N2 11.75(3).

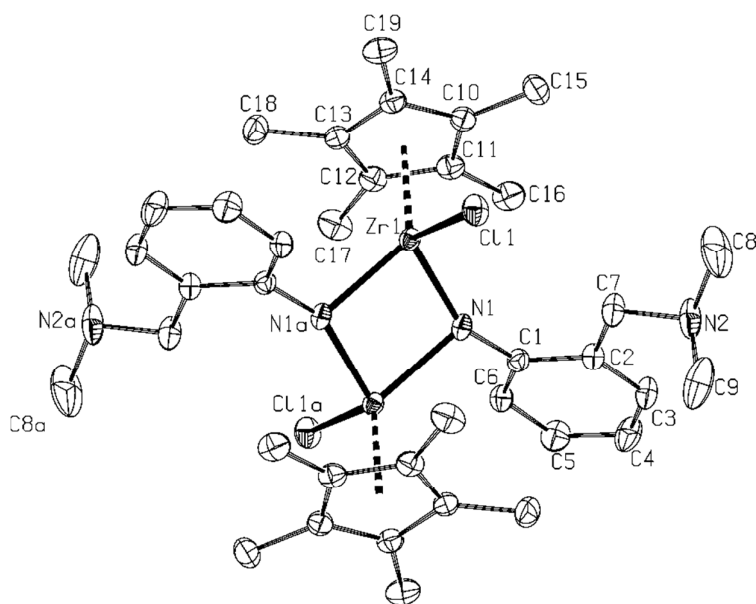


Figure 9. Molecular structure of **16** (ORTEP view, 50% probability level, Symmetry code: (a) $-x, -y+1, -z+1$). Hydrogen atoms are omitted (except of H1) for clarity. Selected interatomic distances [Å] and angles [°]: Zr1–N1 2.0024(19), Zr1–N1a 2.1427(19), Zr1–Cl1 2.4471(6), Zr1–Zr1a 3.1045(5), Cg1–Zr1 2.200(6), N1–Zr1–N1a 83.06(8), N1–Zr1–Cl1 105.72(5), N1–Zr1–Cl1 112.97(5), N1–Zr1–Zr1a 43.25(5), N1a–Zr1–Zr1a 39.81(5), Cl1–Zr1–Zr1a 116.370(18), Cg–Zr1–Zr1a 131.90(11), Cg–Zr1–Cl1 111.02(12).

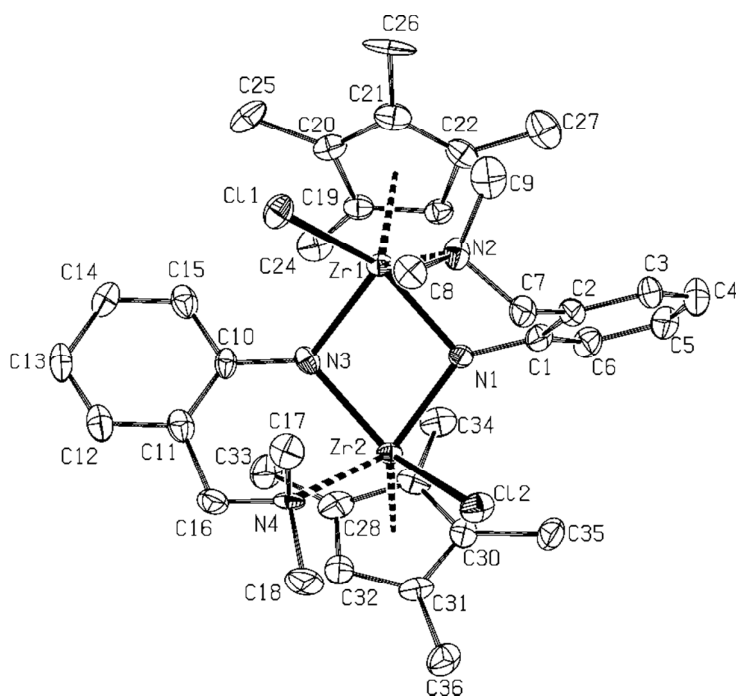


Figure 10. Molecular structure of **15** (ORTEP view, 50% probability level). Hydrogen atoms are omitted for clarity. Selected interatomic distances [Å] and angles [°]: Zr1–N3 2.090(7), Zr1–N1 2.111(7), Zr1–Cl1 2.512(2), Zr1–N2 2.569(7), Zr1–Zr2 3.2352(12), Zr2–N1 2.060(7), Zr2–N3 2.123(7), Zr2–N4 2.447(7), Cg1–Zr1 2.297(5), Cg2–Zr2 2.259(5), N3–Zr1–N1 78.2(3), N3–Zr1–Cl1 88.7(2), N1–Zr1–Cl1 143.69(19), N3–Zr1–N2 120.9(3), N1–Zr1–N2 79.4(3), Cl1–Zr1–N2 78.74(17), Cg1–Zr1–Cl1 103.22(12), Cg2–Zr2–Cl2 106.92(11), Cg1–Zr1–Zr2 131.28(9), Cg2–Zr2–Zr1 134.58(13), C3–C2–C7–N2 62.21(13), C12–C11–C16–N4 19.25(13).

The last complex under structural investigation **17** is the compound containing four different ligands - Cp', *N,N'*-chelating (L^{NN}), *C,N*-chelating (L^{CN}) and chloro ones, accommodated in the coordination polyhedra of the central hafnium atom. Only the L^{CN} ligand is doubly coordinated/covalently bound to the metal with the metal to carbon and nitrogen distances within the range of sum of van der Waals and covalent radii, respectively. The amido function from the potentially *N,N'*-chelating ligand, both chelators from the *C,N*-chelating ligand as well as the chloro ligand are located within the basal plane of the deformed square pyramid, while the fifth substituent is the Cp' ligand on the top of it. All the distances are slightly longer than in both studied mono- and dinuclear complexes but comparable to the sterically hindered complex $Cp^*Hf(L^N)_3$.¹⁸

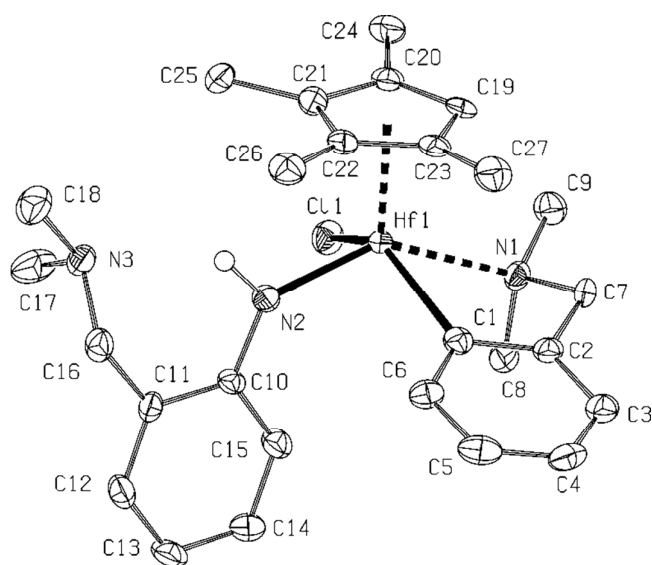


Figure 11. Molecular structure of **17** (ORTEP view, 50% probability level). Hydrogen atoms are omitted (except of H2) for clarity. Selected interatomic distances [Å] and angles [°]: Hf1–N2 2.055(4), Hf1–C1 2.276(5), Hf1–Cl1 2.4440(13), Hf1–N1 2.463(4), Cg1–Hf1 2.194(4), N2–Hf1–C1 90.01(17), N2–Hf1–Cl1 91.14(11), C1–Hf1–Cl1 133.62(12), N2–Hf1–N1 141.65(15), C1–Hf1–N1 70.87(15), Cl1–Hf1–N1 80.15(10), Cg1–Hf1–Cl1 115.19(12), Cg1–Hf1–N2 106.15(11), C3–C2–C7–N1 30.31(9), N2–H2...N3 2.960(5).

Experimental

General Experimental

All operations were carried out under an argon atmosphere using standard Schlenk techniques. ^1H (300.0 MHz), $^{13}\text{C}\{^1\text{H}\}$ (75.4 MHz) NMR spectra were recorded on a Varian Mercury 300 spectrometer at 298 K, if not otherwise stated. Some ^1H (500.13 MHz) NMR spectra were recorded on a Bruker Avance III 500 spectrometer, equipped with a z-gradient 5 mm ProdigyTM cryoprobe. Chemical shifts (δ /ppm) are given relative to solvent signals C_6D_6 : δ_{H} 7.15 ppm, δ_{C} 128.00 ppm; toluene- d_8 : δ_{H} (CH_2D signal) 2.08 ppm, δ_{C} (CD_3 signal) 20.43 ppm; CDCl_3 : δ_{H} 7.26 ppm, δ_{C} 77.16 ppm; CD_2Cl_2 : δ_{H} 5.32 ppm, δ_{C} 53.84 ppm, $\text{C}_6\text{D}_5\text{Br}$: δ_{H} 7.30 ppm, δ_{C} 122.54 ppm. EI-MS spectra were measured on a VG-7070E mass spectrometer at 70 eV. IR spectra of samples in KBr pellets were measured in an air-protecting cuvette on a Nicolet Avatar FT IR spectrometer in the range 400–4000 cm^{-1} . KBr pellets were prepared in a glovebox Labmaster 130 (mBraun) under purified nitrogen. Elemental analyses were carried out on a FLASH EA1112 CHN/O Automatic Elemental Analyzer (Thermo Scientific).

Chemicals

The solvents THF, hexane, and toluene were dried by distillation from sodium/benzophenone and stored over sodium mirror. $(\eta^5\text{-C}_5\text{Me}_5)\text{MCl}_3$ (M = Ti, Zr, Hf) were purchased from Sigma Aldrich and used directly as obtained. $(\eta^5\text{-C}_5\text{Me}_4\text{R})\text{L}^{\text{CN}}\text{MCl}_2$ (M = Zr, Hf; R = Me, H; $\text{L}^{\text{CN}} = \text{C}_6\text{H}_4\text{-2-(CH}_2\text{NMe}_2)\text{-}\mu^2\text{-C,N}$) were synthesized according to a published procedure.²³ Lithium salts of 2,6-Diisopropylaniline $\text{Li}[\text{NHC}_6\text{H}_3\text{-2,6-(CHMe}_2)_2]$ ($\text{L}^{\text{N}}\text{Li}$) and 2-[(dimethylamino)methyl] aniline $\text{Li}[\text{NHC}_6\text{H}_4\text{-2-(CH}_2\text{NMe}_2)]$ ($\text{L}^{\text{NN}}\text{Li}$) were obtained by published methods.²⁹

X-Ray Crystallography

The X-ray data obtained from crystals for all compounds were acquired at 150K using an Oxford Cryostream low-temperature device on a Nonius KappaCCD diffractometer with MoK α radiation ($\lambda = 0.71073\text{\AA}$), a graphite monochromator, and in the Φ and χ scan mode. Data reductions were performed with DENZO-SMN.³⁰ The absorption was corrected by integration methods.³¹ Structures were solved by direct methods (Sir92)³² and refined by full matrix least-square based on F^2 (SHELXL97).³³ Hydrogen atoms were mostly localized on a difference Fourier map, but in order to ensure uniformity of the treatment of the crystal, all hydrogen atoms were recalculated into idealized positions (riding model) and assigned temperature factors $H_{\text{iso}}(\text{H}) = 1.2 U_{\text{eq}}$ (pivot atom) or of $1.5U_{\text{eq}}$ for the methyl moiety with C–H = 0.96, 0.97, 0.98 and 0.93 \AA for methyl, methylene, methine and hydrogen atoms in aromatic rings, or multiply bounded C–H groups respectively. Some of the hydrogen atoms attached to N atoms were located on the Fourier difference map while the other ones were added with bond length of 0.89 \AA . Structures of **3**, **4**, **5**, **8'** are disordered and the disorder was treated by standard procedures of SHELXL program splitting some atoms into two parts.

There are solvent accessible voids within the crystals of **8**. The PLATON /SQUEZZE³⁴ procedures were applied in order to correct these voids and the presence of one molecule of toluene has been evaluated within the unit cell.

Crystallographic data for structural analysis have been deposited with the Cambridge Crystallographic Data Centre. Copies of this information may be obtained free of charge from The Director, CCDC, 12 Union Road, Cambridge CB2 1EY, UK (fax: +44-1223-336033; e-mail: deposit@ccdc.cam.ac.uk or www: <http://www.ccdc.cam.ac.uk>). CCDC deposition numbers CCDC 1044550-1044564. CCDC 1044550 (**3**), CCDC 1044551 (**4**), CCDC 1044552 (**5**), CCDC 1044553 (**7**), CCDC 1044554 (**8'**), CCDC 1044555 (**8**), CCDC 1044556 (**10**), CCDC 1044557 (**11**), CCDC 1044558 (**12**), CCDC 1044559 (**13**), CCDC 1044560 (**14**), CCDC 1044561 (**15**), CCDC 1044562 (**16**), CCDC 1044563 (**17**), CCDC 1044564 (**6**) contain the supplementary crystallographic data for this paper. These data can be obtained free of charge from The Cambridge Crystallographic Data Centre via www.ccdc.cam.ac.uk/data_request/cif.

Synthesis of compounds

*General procedure for the preparation of Li[NHC₆H₃-2,6-ⁱPr₂] (**1**) and Li[NHC₆H₄-2-(CH₂NMe₂)] (**2**)*

The solution of 25 mmol of 2,6-diisopropylaniline ($L^N H$) (4.4 g) or 2-[(dimethylamino)methyl]aniline ($L^{NN} H$) (3.8 g) in 50 ml of toluene was cooled to $-40^\circ C$ and 27.5 mmol of $nBuLi$ (17.2 ml of 1.6 M solution in hexanes) was added using a steel capillary. The precipitated white suspension was stirred 1 h, all liquid components were removed and the white solid was several times washed with hexane and dried in vacuum. Yield: 4.3 g for **1** (94%) or 3.6 g for **2** (92%). The identity and purity of compounds **1** and **2** were identified by 1H NMR spectroscopy.

$L^N Li$ (**1**)

1H NMR (500.13 MHz, 295 K, THF- d_8) δ : 1.19 (d, $^3J_{HH} = 6.8$ Hz, 12H, Me), 2.70 (br s, 1H, NH), 3.19 (br s, 2H, CH), 6.05 (br s, 1H, ArH), 6.68 (br s, 2H, ArH).

$L^{NN} Li$ (**2**)

1H NMR (500.13 MHz, 295 K, C_6D_6) δ : 1.70 (s, 6H, Me_2), 2.73 (s, 1H, NH), 2.97 (br s, 2H, CH_2), 6.48 (t, $^3J_{HH} = 7.2$ Hz, 1H, ArH), 6.60 (d, $^3J_{HH} = 7.1$ Hz, 1H, ArH), 6.79 (d, $^3J_{HH} = 6.8$ Hz, 1H, ArH), 7.13 (t, $^3J_{HH} = 7.2$ Hz, 1H, ArH).

General procedure for the synthesis of complexes 3 - 5

The suspension of 3.0 mmol of **1** (0.55 g) in 15 ml of toluene was cooled to $-40^\circ C$ and solution of 3.0 mmol of $(\eta^5-C_5Me_5)MCl_3$ ($M = Ti$ (0.87 g), Zr (1.00 g), Hf (1.26 g)) in 15 ml of toluene was added using a steel capillary. The mixture was stirred and refluxed for 6 h. Upon concentration of toluene solution to 5 ml, filtration from white powder of LiCl and cooling down to $-18^\circ C$, crystalline suspensions were obtained. The microcrystals were several times washed by hexane to remove organic impurities like 2,6-diisopropylaniline and recrystallized from toluene.

$(\eta^5-C_5Me_5)\{NHC_6H_3-2,6-iPr_2\}TiCl_2$ (**3**)

Yellow crystals. 1H NMR (300 MHz, toluene- d_8) δ : 1.26 (d, $^3J_{HH} = 6.6$ Hz, 12 H, $CHMe_2$), 2.07 (s, 15 H, C_5Me_5), 3.68 (septet, $^3J_{HH} = 6.6$ Hz, 2 H, $CHMe_2$), 6.90 – 7.10 (m, 3 H, C_6H_3), 9.51 (br s, 1 H, NH). $^{13}C\{^1H\}$ NMR (toluene- d_8) δ : 13.3 (C_5Me_5), 24.0 ($CHMe_2$), 28.7 ($CHMe_2$), 124.2, 126.4 ($2 \times C_6H_3CH$), 133.8 (C_5Me_5), 137.1 ($C-CHMe_2$), 140.3 ($C-NH$).

$(\eta^5\text{-C}_5\text{Me}_5)\{\text{NHC}_6\text{H}_3\text{-2,6-}^i\text{Pr}_2\}\text{ZrCl}_2$ (**4**)

Light orange crystals, yield 0.8 g (56%). ^1H NMR (300 MHz, toluene- d_8) δ : 1.20 (d, $^3J_{\text{HH}} = 6.8\text{Hz}$, 12 H, CHMe_2), 1.88 (s, 15 H, C_5Me_5), 3.23 (septet, $^3J_{\text{HH}} = 6.8\text{Hz}$, 2H, CHMe_2), 6.37 (br s, 1H, NH), 7.01 – 7.10 (m, 3H, C_6H_3). $^{13}\text{C}\{^1\text{H}\}$ NMR (toluene- d_8) δ : 11.7 (C_5Me_5), 23.4 (CHMe_2), 29.7 (CHMe_2), 123.0 (C_6H_3), 124.8 (C_5Me_5), 138.6 (C – CHMe_2), 147.5 (C – NH). IR (KBr, cm^{-1}): 3352 (w), 3061 (w), 2961 (vs), 2920 (s), 2869 (s), 1622 (m), 1460 (s), 1430 (s), 1380 (m), 1360 (m), 1322 (m), 1263 (m), 1176 (m), 1113 (w), 1094 (w), 1057 (m), 1044 (w), 1025 (m), 930 (w), 887 (w), 836 (w), 799 (m), 750 (s), 687 (m), 634 (m), 609 (m), 590 (m), 531 (m), 470 (w), 444 (w). M.p. = 120 – 125 °C. Anal. Calc. for $\text{C}_{22}\text{H}_{33}\text{NCl}_2\text{Zr}$: C, 55.79; H, 7.02; N, 2.96. Found: C, 55.71; H, 6.98; N, 2.93.

 $(\eta^5\text{-C}_5\text{Me}_5)\{\text{NHC}_6\text{H}_3\text{-2,6-}^i\text{Pr}_2\}\text{HfCl}_2$ (**5**)

Pale yellow crystals, yield 1.1 g (65%). ^1H NMR (300 MHz, toluene- d_8) δ : 1.20 (d, $^3J_{\text{HH}} = 6.8\text{Hz}$, 12 H, CHMe_2), 1.92 (s, 15 H, C_5Me_5), 3.30 (septet, $^3J_{\text{HH}} = 6.8\text{Hz}$, 2H, CHMe_2), 6.02 (br s, 1H, NH), 6.96 – 7.08 (m, 3H, C_6H_3). $^{13}\text{C}\{^1\text{H}\}$ NMR (toluene- d_8) δ : 11.4 (C_5Me_5), 23.5 (CHMe_2), 29.3 (CHMe_2), 123.0 (C_5Me_5), 123.2 ($m\text{-CH}$, C_6H_3), 125.6 ($p\text{-CH}$, C_6H_3), 142.7 (C – NH), 143.4 (C – CHMe_2). IR (KBr, cm^{-1}): 3355 (w), 3062 (w), 2962 (vs), 2922 (s), 2870 (s), 1622 (m), 1437 (s), 1460 (s), 1381 (s), 1360 (m), 1321 (m), 1263 (m), 1220 (m), 1181 (m), 1113 (m), 1094 (w), 1057 (w), 1044 (w), 1027 (w), 957 (w), 929 (w), 886 (w), 841 (m), 799 (s), 750 (vs), 689 (w), 649 (w), 622 (m), 533 (w), 495 (w), 444 (w). M.p. = 142 – 144 °C. Anal. Calc. for $\text{C}_{22}\text{H}_{33}\text{NCl}_2\text{Hf}$: C, 47.11; H, 5.93; N, 2.50. Found: C, 47.05; H, 5.89; N, 2.44.

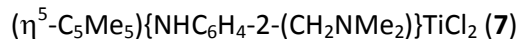
 $(\eta^5\text{-C}_5\text{Me}_5)\{\text{NHC}_6\text{H}_4\text{-2-(CH}_2\text{NMe}_2)\}_3\text{Zr}$ (**6**)

Only several crystals of compound **6** were isolated as a side product during preparation of **4**. For crystal structure of **6** see Figure 4. Similar structures are known for -NHR R = ^tBu ; 2,4,6- $\text{Me}_3\text{C}_6\text{H}_2$ and 2,6- $^i\text{Pr}_2\text{C}_6\text{H}_3$ ligands.¹⁸

General procedure for the synthesis of complexes 7 - 9

The suspension of 3.0 mmol of **2** (0.47 g) in 15 ml of toluene was cooled to -40° C and solution of 3.0 mmol of $(\eta^5\text{-C}_5\text{Me}_5)\text{MCl}_3$ (M=Ti (0.87 g), Zr (1.00 g), Hf (1.26 g)) in 15 ml of toluene was added using a steel capillary. The mixture was stirred overnight. Upon

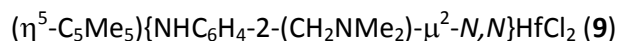
concentration of toluene solution to 5 ml, filtration from white powder of LiCl and cooling down crystalline suspensions were obtained. Crystals were several times washed by hexane to remove organic impurities and recrystallized from toluene.



Red crystals, yield 0.67 g (55%). ^1H NMR (300 MHz, CDCl_3) δ : 2.28 (s, 15 H, C_5Me_5), 2.35 (s, 6 H, NMe_2), 3.56 (s, 2 H, CH_2NMe_2), 6.76 – 6.82, 6.93 – 6.97, 7.24 – 7.30, 7.77 – 7.80 (4 x m, 4 x 1H, CH, C_6H_4), 12.45 (br s, 1H, NH). $^{13}\text{C}\{^1\text{H}\}$ NMR (CDCl_3) δ : 13.2 (C_5Me_5), 44.8 (NMe_2), 63.7 (CH_2NMe_2), 119.0 (C – CH_2 , C_6H_4), 122.1, 123.6, 129.1 (3x CH, C_6H_4), 129.4 (C_5Me_5), 129.6 (CH, C_6H_4), 154.4 (C – N, C_6H_4). IR (KBr, cm^{-1}): 2958 (m), 2912 (m), 2857 (m), 2822 (m), 2776 (m), 1589 (m), 1573 (w), 1553 (w), 1485 (s), 1467 (s), 1380 (m), 1316 (s), 1249 (s), 1229 (m), 1177 (w), 1153 (w), 1099 (m), 1022 (m), 962 (m), 936 (w), 885 (w), 864 (w), 845 (w), 796 (m), 759 (s), 721 (w), 661 (w), 621 (w), 537 (w), 520 (w), 472 (w), 450 (m). M.p. = 152 °C. Anal. Calc. for $\text{C}_{19}\text{H}_{28}\text{N}_2\text{Cl}_2\text{Ti}$: C, 56.60; H, 7.00; N, 6.95. Found: C, 56.54; H, 6.95; N, 6.91.



Yellow crystals, yield 0.87 g (65%). ^1H NMR (300 MHz, 238 K, toluene- d_8) δ : 1.91 (s, 15 H, C_5Me_5), 2.17 (s, 3 H, NMe_2), 2.51 (d, 1 H, $^2J_{\text{HH}} = 13.3\text{Hz}$, CH_2NMe_2), 2.72 (s, 3 H, NMe_2), 5.00 (d, 1 H, $^2J_{\text{HH}} = 13.3\text{Hz}$, CH_2NMe_2), 6.15 – 6.23 (m, 1H, CH, C_6H_4), 6.51 – 6.61 (m, 2H, CH, C_6H_4), 6.82 – 7.01 (m, 1H, CH, C_6H_4), 7.34 (br s, 1H, NH). $^{13}\text{C}\{^1\text{H}\}$ NMR (238 K, toluene- d_8) δ : 12.2 (C_5Me_5), 46.5, 51.3 (2x NMe_2), 64.0 (CH_2NMe_2), 116.7, 119.4, 123.8, 129.4, 130.5 (CH and C – CH_2 and C_6H_4), 123.4 (C_5Me_5), 150.6 (C_6H_4 , C – N). IR (KBr, cm^{-1}): 3376 (m), 3023 (m), 2985 (m), 2908 (s), 2866 (m), 1936 (w), 1897 (w), 1859 (w), 1824 (w), 1786 (w), 1598 (s), 1585 (s), 1495 (s), 1476 (m), 1455 (s), 1428 (s), 1403 (m), 1379 (s), 1358 (m), 1313 (s), 1281 (s), 1246 (s), 1192 (m), 1175 (w), 1158 (w), 1145 (w), 1108 (m), 1067 (w), 1048 (m), 1020 (m), 993 (m), 965 (w), 931 (w), 889 (m), 858 (w), 838 (m), 798 (m), 755 (s), 721 (m), 696 (w), 640 (m), 614 (m), 544 (m), 488 (w), 452 (w), 410 (w). M.p. = 150 °C. Anal. Calc. for $\text{C}_{19}\text{H}_{28}\text{N}_2\text{Cl}_2\text{Zr}$: C, 51.10; H, 6.32; N, 6.27. Found: C, 51.01; H, 6.22; N, 6.21.



Yellow crystals, yield 1.09 g (68%). ^1H NMR (300 MHz, 228 K, toluene- d_8) δ : 1.95 (s, 15 H, C_5Me_5), 2.15, 2.66 (2 x s, 3 H, NMe_2), 2.47, 4.93 (2 x d, 1 H, $^2J_{\text{HH}} = 13.3\text{Hz}$, CH_2NMe_2), 6.26 – 6.38 (m, 1 H, CH, C_6H_4), 6.45 (br s, 1 H, NH), 6.58 – 6.72 (m, 2 H, CH, C_6H_4), 7.04 – 7.14 (m, 1 H, CH, C_6H_4). $^{13}\text{C}\{^1\text{H}\}$ NMR (228 K, toluene- d_8) δ : 12.3 (C_5Me_5), 46.7, 51.4 ($2\times \text{NMe}_2$), 63.8 (CH_2NMe_2), 117.8, 119.1, 121.2, 123.5, 129.9 (CH and C – CH_2 and C_6H_4), signal C_5Me_5 is overlapped by solvent signal, 150.4 (C_6H_4 , C-N). IR (KBr, cm^{-1}): 3270 (w), 2858 (s), 2816 (m), 2773 (m), 1600 (s), 1486 (s), 1458 (s), 1427 (m), 1401 (w), 1378 (m), 1363 (m), 1315 (m), 1272 (s), 1253 (s), 1179 (w), 1148 (w), 1108 (m), 1044 (w), 1018 (m), 985 (w), 927 (w), 891 (m), 832 (w), 800 (m), 752 (s), 730 (m), 695 (m), 640 (w), 608 (w), 591 (w), 546 (w), 488 (w), 466 (w). M.p. = 150 °C. Anal. Calc. for $\text{C}_{19}\text{H}_{28}\text{N}_2\text{Cl}_2\text{Hf}$: C, 42.75; H, 5.29; N, 5.25. Found: C, 42.71; H, 5.22; N, 5.19.

$[(\eta^5\text{-C}_5\text{Me}_5)\{\mu\text{-NC}_6\text{H}_4\text{-2-(CH}_2\text{NMe}_2)\}\text{HfCl}]_2$ (**10**)

Only several crystals of compound **10** were isolated as a side product during preparation of **9**. No other analyses could have been performed due to low amount and decomposition of the sample during X-ray analysis. For crystal structure of **10** see Figure 8.

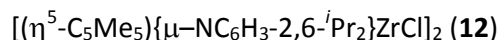
General procedure for the synthesis of complexes 11 - 14

The suspension of 3.0 mmol of **1** (0.55 g) in 15 ml of toluene was cooled to -40°C and a solution of 3.0 mmol of $(\eta^5\text{-C}_5\text{Me}_4\text{R})\text{L}^{\text{CN}}\text{MCl}_2$ (R=H, M=Zr (1.25 g), R=Me, M=Zr (1.30 g), R=H, M=Hf (1.51 g), R=Me, M=Hf (1.56 g)) in 15 ml of toluene was added using a steel capillary. When warmed to room temperature colour change was observed from red colour to light brown. The mixture was stirred and refluxed for 4 h. Upon concentration of toluene solution to 5 ml, filtration from white powder of LiCl and cooling down crystalline suspensions were obtained. Solid material was isolated, several times washed by hexane, and dried under vacuum. Coloured crystals were obtained after recrystallization from toluene.

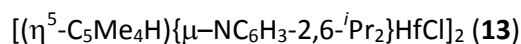
$[(\eta^5\text{-C}_5\text{Me}_4\text{H})\{\mu\text{-NC}_6\text{H}_3\text{-2,6-}^i\text{Pr}_2\}\text{ZrCl}]_2$ (**11**)

Light orange crystals, yield 1.95 g (77%). ^1H NMR (300 MHz, C_6D_6) δ : 1.31, 1.39 ($2\times \text{d}$, $^3J_{\text{HH}} = 6.5\text{Hz}$, 12 H, CHMe_2), 1.57, 2.13 (2 x s, 12H, C_5Me_4), 4.24 (septet, $^3J_{\text{HH}} = 6.7\text{Hz}$, 4 H, CHMe_2), 5.72 (s, 2H, HC_5Me_4), 7.02 – 7.13 (m, 6 H, C_6H_3). $^{13}\text{C}\{^1\text{H}\}$ NMR (C_6D_6) δ : 10.9, 13.1 ($2\times \text{C}_5\text{Me}_4$),

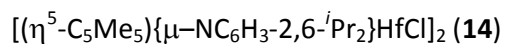
25.8, 28.1 (2× CHMe₂), 28.5 (CHMe₂), 113.5 (CH, C₅Me₄H), 124.3 (CH, C₆H₃), 125.4, 125.4 (2× C_{ipso}, C₅Me₄H), 144.1 (C – CHMe₂, C₆H₃), 145.5 (C – N, C₆H₃). IR (KBr, cm⁻¹): 3052 (m), 2973 (s), 2938 (s), 2915 (s), 2869 (m), 2729 (w), 1914 (w), 1623 (w), 1585 (w), 1505 (w), 1495 (m), 1412 (s), 1359 (m), 1384 (m), 1317 (m), 1238 (m), 1144 (m), 1169 (vs), 1109 (s), 1097 (m), 1042 (w), 985 (w), 926 (w), 887 (s), 863 (s), 818 (s), 797 (m), 750 (vs), 707 (m), 631 (w), 613 (w), 588 (w), 556 (s), 483 (s), 452 (w), 406 (m). M.p. = 243 °C. Anal. Calc. for C₄₂H₆₀N₂Cl₂Zr₂: C, 59.61; H, 7.15; N, 3.31. Found: C, 59.53; H, 7.08; N, 3.29.



Light orange crystals, yield 1.86 g (71%), ¹H-NMR (300 MHz, toluene-*d*₈) δ: 1.22, 1.47 (2× d, ³J_{HH} = 6.4Hz, 12 H, CHMe₂), 1.76 (s, 30H, C₅Me₅), 4.25 (septet, ³J_{HH} = 6.4Hz, 4 H, CHMe₂), 6.94 (t, ³J_{HH} = 7.5Hz, 2H, C₆H₃), 7.06 (d, ³J_{HH} = 7.5Hz, 4H, C₆H₃). ¹³C{¹H} NMR (toluene-*d*₈) δ: 11.7 (C₅Me₅), 25.4, 28.5 (2× CHMe₂), 30.4 (CHMe₂), 124.0 (C₅Me₅), 124.7 (CH, C₆H₃), 141.6 (C – CHMe₂, C₆H₃), 148.2 (C – N, C₆H₃). IR (KBr, cm⁻¹) 3052 (w), 2978 (s), 2953 (s), 2915 (s), 2871 (m), 1588 (w), 1458 (m), 1413 (m), 1381 (m), 1360 (w), 1318 (w), 1294 (w), 1250 (w), 1228 (w), 1162 (s), 1143 (s), 1100 (s), 1039 (w), 1025 (w), 926 (w), 885 (m), 854 (m), 797 (w), 751 (s), 705 (w), 624 (w), 611 (w), 599 (w), 556 (s), 482 (s), 414 (m). M.p. = 240 °C. Anal. Calc. for C₄₄H₆₄N₂Cl₂Zr₂: C, 60.44; H, 7.38; N, 3.20. Found: C, 60.38; H, 7.31; N, 3.16.



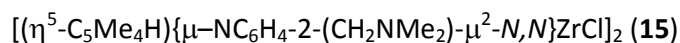
Yellow crystals, yield 2.50 g (82%), ¹H NMR (300 MHz, toluene-*d*₈) δ: 1.26, 1.42 (2× d, ³J_{HH} = 6.6Hz, 12 H, CHMe₂) 2.04, 2.19 (2×s, 12H, C₅Me₄), 4.35 (septet, ³J_{HH} = 6.6Hz, 4 H, CHMe₂), 5.72 (s, 2H, HC₅Me₄), 6.86 – 6.92 (m, 2H, C₆H₃), 7.07 – 7.11 (m, 4H, C₆H₃). ¹³C{¹H} NMR (toluene-*d*₈) δ: 10.9, 13.1 (2× C₅Me₄), 26.1(CHMe₂), 28.0 (CHMe₂), 29.0 (CHMe₂), 112.5 (CH, C₅Me₄H), 122.6, 122.9 (2× C_{ipso}, C₅Me₄H), 124.2, 128.2 (2× CH, C₆H₃), 143.0 (C – CHMe₂), 146.0 (C – N, C₆H₃). IR (KBr, cm⁻¹) 3053 (w), 2981 (m), 2968 (m), 2949 (m), 2938 (m), 2915 (m), 2869 (w), 1460 (w), 1414 (m), 1384 (w), 1359 (w), 1318 (w), 1296 (w), 1237 (w), 1169 (s), 1144 (w), 1108 (m), 1097 (w), 1037 (w), 887 (m), 867 (w), 821 (m), 798 (w), 751 (s), 708 (w), 612 (w), 568 (s), 496 (m), 452 (w), 407 (w). M.p. = 263 °C. Anal. Calc. for C₄₂H₆₀N₂Cl₂Hf₂: C, 49.42; H, 5.92; N, 2.74. Found: C, 49.32; H, 5.84; N, 2.71.



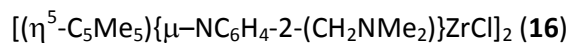
Synthesized according to procedures published elsewhere.⁸ Yellow crystals, yield 2.23 g (71%).

General procedure for the synthesis of complexes 15 and 16

The suspension of 0.5 mmol of **2** (0.078 g) in 15 ml of toluene was cooled to -70° C and solution of 0.5 mmol of $(\eta^5\text{-C}_5\text{Me}_4\text{R})\text{L}^{\text{CN}}\text{ZrCl}_2$ (R=H (0.21 g); R=Me (0.22 g)) in 15 ml of toluene was added using a steel capillary. The mixture was stirred and refluxed for 4 h. Upon concentration of toluene solution to 5 ml and filtration from a white powder of LiCl, all volatiles were removed under vacuum. Solid residue was dissolved in toluene and crystallized at -18° C. Coloured crystals were washed by small volumes of hexane and isolated.



Orange crystals; yield 0.18 g (45 %). ¹H NMR (300 MHz, C₆D₅Br) δ : 1.48, 1.72, 2.15, 2.28 (4× s, 3 H, C₅Me₄), 2.32 (br s, 6 H, NMe₂), 3.12, 3.95 (2× d, ²J_{HH} = 13.5 Hz, 1 H, CH₂), 5.80 (s, 1 H, C₅Me₄H), 6.51–7.37 (m, 4 H, C₆H₄). ¹³C{¹H} NMR(C₆D₅Br) δ : 11.8, 13.0, 13.7, 14.6 (4× C₅Me₄), 50.8 (br s, NMe₂), 67.1 (CH₂), 115.3 (C₅Me₄H CH), 119.3 (C₆H₄ CH), 121.8, 124.1, 124.8 (3× C₅Me₄ C_{ipso}), 125.6, 128.3 (2× C₆H₄ CH), 155.0 (C₆H₄ C-N) ppm; signals due to C₆H₄ C-CH₂, C₅Me₄ C_{ipso} (both around 122.6 ppm) and C₆H₄ CH (around 129.7 ppm) obscured by the solvent signals. IR (KBr, cm⁻¹): 2909(m), 1591(m), 1561(w), 1471(s), 1446(m), 1370(w) 1263(s), 1232(vs) 983(w), 894(m), 798(w), 755(m), 587(s), 539(w), 444(w). M.p. = 240 °C. Anal. Calc. for C₃₆H₅₀Cl₂Zr₂N₄: C, 54.58; H, 6.35; N, 7.07. Found: C, 54.49; H, 6.29; N, 7.01.



Orange crystals; yield 0.21 g (51 %).

Tentatively assigned as 2 isomers (2:1).

major isomer, ¹H NMR (300 MHz, toluene-*d*₈): δ 1.75 (s, 15 H, C₅Me₅), 2.40 (s, 6 H, NMe₂), 3.47, 3.58 (2× d, ²J_{HH} = 15.3 Hz, 1 H, CH₂), 6.83-7.62 (m, C₆H₄ overlapping with the other isomer) ppm. ¹³C{¹H} NMR (toluene-*d*₈): δ 11.2 (C₅Me₅), 47.3 (NMe₂), 63.0 (CH₂), 121.6, 122.7 (2× C₆H₄ CH), 123.3 (C₅Me₅), 127.5, 130.3 (2× C₆H₄ CH), 130.5 (C₆H₄ C-CH₂), 150.2 (C₆H₄ C-N)

ppm. **minor isomer**, ^1H NMR (300 MHz, toluene- d_8): δ 1.78 (s, 15 H, C_5Me_5), 2.45 (s, 6 H, NMe_2), 3.66, 3.77 (2 \times d, $^2J = 15.5$ Hz, 1 H, CH_2), 6.83-7.62 (m, C_6H_4 overlapping with the other isomer) ppm. $^{13}\text{C}\{^1\text{H}\}$ NMR (toluene- d_8): δ 11.6 (C_5Me_5), 47.5 (NMe_2), 63.2 (CH_2), 120.2, 123.4 (2 \times C_6H_4 CH), 125.8 (C_5Me_5), 126.3, 131.2 (2 \times C_6H_4 CH), 132.5 (C_6H_4 C- CH_2), 148.1 (C_6H_4 C-N) ppm. IR (KBr, cm^{-1}): 3054(w), 2975(m), 2941(m), 2907(s), 2858(m), 2816(m) 2771(m), 1588(m) 1563(m), 1471(s), 1441(s), 1379(m), 1363(m), 1267(s), 1230(vs), 1172(w), 1148(w), 1097(w), 1032(m), 986(w), 936(w), 894(m) 854(m), 798(w), 761(vs), 735(w), 721(w), 635(m), 578(s), 546(w), 507(w), 484(m), 433(m). M.p. = 280 °C. Anal. Calc. for $\text{C}_{38}\text{H}_{54}\text{Zr}_2\text{Cl}_2\text{N}_4$: C, 55.64; H, 6.64; N, 6.83. Found: C, 55.58; H, 6.59; N, 6.78.

*Preparation of $(\eta^5\text{-C}_5\text{Me}_4\text{H})\{\text{NHC}_6\text{H}_4\text{-2-(CH}_2\text{NMe}_2)\}\{\text{C}_6\text{H}_4\text{-2-(CH}_2\text{NMe}_2)\text{-}\mu^2\text{-C,N}\}\text{HfCl}$ (**17**)*

The suspension of 0.5 mmol of **2** (0.078 g) in 15 ml of toluene was cooled to -70°C and solution of 0.5 mmol of $(\eta^5\text{-C}_5\text{Me}_4\text{H})\text{L}^{\text{CN}}\text{HfCl}_2$ (0.25 g) in 15 ml of toluene was added using a steel capillary. The mixture was stirred and refluxed for 4 h. Upon concentration of the toluene solution to 5 ml, filtration from a white powder of LiCl, all volatiles were removed under vacuum. Solid residue was dissolved in toluene and crystallized at -18°C . Colourless crystals were washed by small volumes of hexane and isolated. Yield was 0.18 g (58 %).

^1H NMR (300 MHz, toluene- d_8): δ 1.22 (s, 3 H, C_5Me_4 prox.), 2.09 (s, 6 H, NMe_2 of L^{NN}), 2.17 (s, 3 H, C_5Me_4 dist.), 2.26 (s, 3 H, C_5Me_4 prox.), 2.27 (s, 3 H, C_5Me_4 dist.), 2.37, 2.39 (2 \times br s, 3 H, NMe_2 of L^{CN}), 3.01 (d, $^2J_{\text{HH}} = 13.7$ Hz, 1 H, CH_2 of L^{CN}), 3.30, 3.45 (2 \times d, $^2J_{\text{HH}} = 12.3$ Hz, 1 H, CH_2 of L^{NN}), 3.77 (d, $^2J_{\text{HH}} = 13.7$ Hz, 1 H, CH_2 of L^{CN}), 5.03 (s, 1 H, $\text{C}_5\text{Me}_4\text{H}$), 6.54-6.61 (m, 1 H, C_6H_4 of L^{NN}), 6.84-7.16 (m, 6 H, C_6H_4 of L^{CN} and L^{NN}), 7.67-7.72 (m, 1 H, C_6H_4 of L^{CN}), 8.71 (NH) ppm. $^{13}\text{C}\{^1\text{H}\}$ NMR (toluene- d_8): δ 11.2, 11.7 (2 \times C_5Me_4 dist.), 13.0, 14.8 (2 \times C_5Me_4 prox.), 44.8 (NMe_2 of L^{NN}), 47.6, 49.2 (NMe_2 of L^{CN}), 64.7 (CH_2 of L^{NN}), 70.3 (CH_2 of L^{CN}), 111.8 ($\text{C}_5\text{Me}_4\text{H}$ CH), 117.8, 119.2 (2 \times C_6H_4 CH of L^{NN}), 120.1, 121.5, 121.7 (3 \times C_5Me_4 C_{ipso}), 123.0 (C_6H_4 C- CH_2 of L^{NN}), 123.6 (C_5Me_4 C_{ipso}), 123.8, 127.1, 127.3 (3 \times C_6H_4 CH of L^{CN}), 128.0, 130.8 (2 \times C_6H_4 CH of L^{NN}), 143.2 (C_6H_4 CH of L^{CN}), 146.9 (C_6H_4 C- CH_2 of L^{CN}), 153.3 (C_6H_4 C-N of L^{NN}), 196.5 (C_6H_4 C-Hf of L^{CN}) ppm. IR (KBr, cm^{-1}): 3276(w), 3043(w), 2914(m), 2855(m), 2816(m) 2773(m), 1616(m) 1600(m), 1572(w), 1486(s), 1458(s), 1363(m), 1272(s), 1254(m), 1177(w), 1148(w), 1099(m), 1043(m), 1018(s), 989(w), 883(m) 839(m), 790(m), 748(vs), 724(m), 645(m),

614(m), 507(w), 430(w)., M.p. = 260 °C, Anal. Calc. for C₂₇H₃₈ClHfN₃: C, 52.43; H, 6.19; N, 6.79. Found: C, 52.38; H, 6.09; N, 6.72.

Preparation of (η^5 -C₅Me₅){NHC₆H₄-2-(CH₂NMe₂)}{C₆H₄-2-(CH₂NMe₂)- μ^2 -C,N}HfCl (**18**)

The suspension of 0.5 mmol of **2** (0.078 g) in 15 ml of toluene was cooled to -70° C and solution of 0.5 mmol of (η^5 -C₅Me₅)L^{CN}HfCl₂ (0.26 g) in 15 ml of toluene was added using a steel capillary. The mixture was stirred and refluxed for 4 h. Upon concentration of the toluene solution to 5 ml, filtration from a white powder of LiCl, all volatiles were removed under vacuum. Solid residue was dissolved in toluene and crystalized at -18° C. Only several yellow crystals of **10** were obtained, isolated and washed by small volumes of hexane.

Hexane was added into toluene solution and formation of white precipitate was observed.

The white powder was isolated and dried under vacuum. Yield was 0.20 g (63 %).

¹H NMR (300 MHz, toluene-*d*₈): δ 1.91 (s, 15 H, C₅Me₅), 2.06 (s, 6 H, NMe₂ of L^{NN}), 2.36, 2.37 (2× br s, 3 H, NMe₂ of L^{CN}), 2.96 (d, ²J_{HH} = 14.3 Hz, 1 H, CH₂ of L^{CN}), 3.26, 3.45 (2× d, ²J_{HH} = 12.2 Hz, 1 H, CH₂ of L^{NN}), 3.86 (d, ²J_{HH} = 14.3 Hz, 1 H, CH₂ of L^{CN}), 6.49-6.57 (m, 1 H, C₆H₄ CH of L^{NN}), 6.78-7.25 (m, 6 H, C₆H₄ of L^{CN} and L^{NN}), 7.73-7.78 (m, 1 H, C₆H₄ of L^{CN}), 8.46 (NH) ppm.

¹³C{¹H} NMR (toluene-*d*₈): δ 12.0 (C₅Me₅), 45.0 (NMe₂ of L^{NN}), 47.9, 48.1 (NMe₂ of L^{CN}), 64.5 (CH₂ of L^{NN}), 70.1 (CH₂ of L^{CN}), 117.7, 119.9 (C₆H₄ CH of L^{NN}), 120.9 (C₅Me₅), 123.4 (C₆H₄ C-CH₂ of L^{NN}), 123.7, 126.6, 126.7, 129.2, 130.8 (C₆H₄ CH), 142.9 (C₆H₄ CH of L^{CN}), 146.0 (C₆H₄ C-CH₂ of L^{CN}), 153.2 (C₆H₄ C-N of L^{NN}), 196.7 (C₆H₄ C-Hf of L^{CN}) ppm. IR (KBr, cm⁻¹): 3235(w), 2912(vs), 2692(w), 1636(w), 1497(m), 1457(s) 1381(m), 1244(s), 983(w), 930(w), 751(vs), 545(m), 457(s). Anal. Calc. for C₂₈H₄₀ClHfN₃: C, 53.16; H, 6.37; N, 6.64. Found: C, 53.08; H, 6.32; N, 6.55.

Conclusions

Two series of mononuclear complexes with terminal Group 4 metal-amide bond(s), and dinuclear complexes with bridging fashion of an imide have been prepared and structurally characterized. All the described reactions were carried out in an equimolar ratio to maintain integrity of the studied reactions. Two different kinds of nitrogen ligands and two Cp ligands with different electronic and steric effects were employed in order to demonstrate variability of the Group 4 metal coordination spheres. The solid-state structural study proved

to be an essential tool for understanding of all ongoing processes. In summary, the amido complexes are monomeric, imido ones with L^N ligand dinuclear. Similar arrangement of the substituents is adopted in cases of hafnium complexes with potentially N,N' -chelating amido ligand (L^{NN}) and also the combination of zirconium complexes with L^{NN} and bulkier Cp^* ligands. The only exception is the dinuclear zirconium complex with L^{NN} and less bulky Cp' ligand, where the rare mutual arrangement of the same type of substituents is *syn* with respect to the central M_2N_2 plane. The results confirm anticipated differences in the chemical behavior and properties of Group 4 metals showing an increasing stability of amido- and imido- complexes from titanium to hafnium.

Supporting Information

Tables of selected crystallographic parameters for **3**, **4**, **5**, **6**, **7**, **8**, **8'**, **10**, **11**, **12**, **13**, **14**, **15**, **16**, **17**. Figures of molecular structure and selected interatomic distances and angles for **3**, **4**, **14**. Eyring plots for **8** and **9**. An expanded region of 1H NMR spectra of **8** in the temperature range from -35 °C to 55 °C.

Acknowledgement

This research was supported by the Czech Science Foundation (Project No. P106/10/0924).

References

1. a) M. H. Chisholm and I. P. Rothwell, in *Comprehensive Coordination Chemistry*, eds. G. Wilkinson, R. D. Gillard and J. A. McCleverty, Pergamon, Oxford, 1987, vol. 2, p. 161 and references therein; b) M. F. Lappert, A. V. Protchenko, P. P. Power and A. L. Seeber, *Metal Amide Chemistry*, John Wiley & Sons, Hoboken, 2008.
2. P. D. Bolton and P. Mountford, *Adv. Synth. Catal.*, 2005, **347**, 355-366.
3. W. A. Nugent and B. L. Haymore, *Coord. Chem. Rev.*, 1980, **31**, 123-175.
4. L. H. Gade and P. Mountford, *Coord. Chem. Rev.*, 2001, **216**, 65-97.
5. D. J. Mindiola, *Acc. Chem. Res.*, 2006, **39**, 813-821.
6. A. R. Fout, U. J. Kilgore and D. J. Mindiola, *Chem. Eur. J.*, 2007, **13**, 9428-9440.

7. Y. H. Li, Y. H. Shi and A. L. Odom, *J. Am. Chem. Soc.*, 2004, **126**, 1794-1803.
8. I. Castillo and T. D. Tilley, *J. Organomet. Chem.*, 2002, **643**, 431-440.
9. C. Lorber, R. Choukroun and L. Vendier, *Eur. J. Inorg. Chem.*, 2006, 4503-4518.
10. a) C. Lorber and L. Vendier, *Inorg. Chem.*, 2011, **50**, 9927-9929; b) C. Lorber and L. Vendier, *Organometallics*, 2010, **29**, 1127-1136.
11. X. G. Yu, S. J. Chen, X. P. Wang, X. T. Chen and Z. L. Xue, *Organometallics*, 2009, **28**, 4269-4275.
12. M. Said, D. L. Hughes and M. Bochmann, *Dalton Trans.*, 2004, 359-360.
13. J. R. Ascenso, C. G. de Azevedo, A. R. Dias, M. T. Duarte, I. Eleuterio, M. J. Ferreira, P. T. Gomes and A. M. Martins, *J. Organomet. Chem.*, 2001, **632**, 17-26.
14. a) Y. I. Bai, M. Noltemeyer and H. W. Roesky, *Z. Naturforsch., B: Chem. Sci.*, 1991, **46**, 1357-1363; b) Y. Bai, H. W. Roesky and M. Noltemeyer, *Z. Anorg. Allg. Chem.*, 1991, **595**, 21-26.
15. a) K. F. Liu, Q. L. Wu, W. Gao and Y. Mu, *Dalton Trans.*, 2011, **40**, 4715-4721; b) K. F. Liu, Q. L. Wu, W. Gao, Y. Mu and L. Ye, *Eur. J. Inorg. Chem.*, 2011, 1901-1909.
16. E. S. Cho, Y. C. Won, S. Y. Lee, B. Y. Lee, D. M. Shin and Y. K. Chung, *Inorg. Chim. Acta*, 2004, **357**, 2301-2308.
17. B. M. Chapin, L. D. Hughs, J. A. Golen, A. L. Rheingold and A. R. Johnson, *Acta Crystallogr., Sect. C: Cryst. Struct. Commun.*, 2010, **66**, M191-M193.
18. Y. N. Bai, H. W. Roesky, M. Noltemeyer and M. Witt, *Chem. Ber. Recl.*, 1992, **125**, 825-831.
19. a) K. H. Thiele, G. A. Hadi, J. Wunderle and H. Langhof, *Z. Kristallogr.*, 1994, **209**, 373-374; b) P. Doufou, K. A. Abboud and J. M. Boncella, *J. Organomet. Chem.*, 2000, **603**, 213-219; c) A. C. Benjamin, A. S. P. Frey, M. G. Gardiner, C. L. Raston, B. W. Skelton and A. H. White, *J. Organomet. Chem.*, 2008, **693**, 776-780; d) V. Taberner, T. Cuenca and E. Herdtweck, *Eur. J. Inorg. Chem.*, 2004, 3154-3162; e) J. E. Bol, B. Hessen, J. H. Teuben, W. J. J. Smeets and A. L. Spek, *Organometallics*, 1992, **11**, 1981-1983; f) K. E. Duplooy, U. Moll, S. Wocadlo, W. Massa and J. Okuda, *Organometallics*, 1995, **14**, 3129-3131.
20. a) W. J. Grigsby, M. M. Olmstead and P. P. Power, *J. Organomet. Chem.*, 1996, **513**, 173-180; b) S. J. Lancaster, S. Al-Benna, M. Thornton-Pett and M. Bochmann, *Organometallics*, 2000, **19**, 1599-1608; c) K. Weitershaus, H. Wadepohl and L. H.

- Gade, *Organometallics*, 2009, **28**, 3381-3389; d) A. Abarca, P. Gomez-Sal, A. Martin, M. Mena, J. M. Poblet and C. Yelamos, *Inorg. Chem.*, 2000, **39**, 642-651; e) K. Kaleta, P. Arndt, T. Beweries, A. Spannenberg, O. Theilmann and U. Rosenthal, *Organometallics*, 2010, **29**, 2604-2609; f) H. Tsurugi, H. Nagae and K. Mashima, *Chem. Commun.*, 2011, **47**, 5620-5622; g) A. K. Hughes, S. M. B. Marsh, J. A. K. Howard and P. S. Ford, *J. Organomet. Chem.*, 1997, **528**, 195-198; h) P. J. Walsh, F. J. Hollander and R. G. Bergman, *J. Am. Chem. Soc.*, 1988, **110**, 8729-8731; i) A. M. Baranger, P. J. Walsh and R. G. Bergman, *J. Am. Chem. Soc.*, 1993, **115**, 2753-2763; j) Z. Li, J. Huang, T. Yao, Y. Qian and M. Leng, *J. Organomet. Chem.*, 2000, **598**, 339-347; k) J. F. Eichler, O. Just and W. S. Rees, *Phosphorus, Sulfur Silicon Relat. Elem.*, 2004, **179**, 715-726; l) G. C. Bai, H. W. Roesky, H. J. Hao, M. Noltemeyer and H. G. Schmidt, *Inorg. Chem.*, 2001, **40**, 2424-+; m) Y. Bai, H. W. Roesky, H. G. Schmidt and M. Noltemeyer, *Z. Naturforsch., B: Chem. Sci.*, 1992, **47**, 603-608; n) J. D. Selby, M. Feliz, A. D. Schwarz, E. Clot and P. Mountford, *Organometallics*, 2011, **30**, 2295-2307.
21. a) J. A. Pool, E. Lobkovsky and P. J. Chirik, *Nature*, 2004, **427**, 527-530; b) J. N. Armor, *Inorg. Chem.*, 1978, **17**, 203-213; c) J. A. Pool, E. Lobkovsky and P. J. Chirik, *J. Am. Chem. Soc.*, 2003, **125**, 2241-2251; d) W. H. Bernskoetter, J. A. Pool, E. Lobkovsky and P. J. Chirik, *J. Am. Chem. Soc.*, 2005, **127**, 7901-7911; e) D. J. Knobloch, E. Lobkovsky and P. J. Chirik, *Nat Chem*, 2010, **2**, 30-35; f) W. H. Bernskoetter, E. Lobkovsky and P. J. Chirik, *J. Am. Chem. Soc.*, 2005, **127**, 14051-14061; g) W. H. Bernskoetter, A. V. Olmos, E. Lobkovsky and P. J. Chirik, *Organometallics*, 2006, **25**, 1021-1027; h) T. E. Hanna, W. H. Bernskoetter, M. W. Bouwkamp, E. Lobkovsky and P. J. Chirik, *Organometallics*, 2007, **26**, 2431-2438; i) M. Hirotsu, P. P. Fontaine, P. Y. Zavalij and L. R. Sita, *J. Am. Chem. Soc.*, 2007, **129**, 12690-+; j) S. P. Semproni, E. Lobkovsky and P. J. Chirik, *J. Am. Chem. Soc.*, 2011, **133**, 10406-10409.
22. a) T. W. Graham, J. Kickham, S. Courtenay, P. R. Wei and D. W. Stephan, *Organometallics*, 2004, **23**, 3309-3318; b) A. Decker, D. Fenske and K. Maczek, *Angew. Chem. Int. Ed.*, 1996, **35**, 2863-2866; c) H. W. Roesky, Y. Bai and M. Noltemeyer, *Angew. Chem. Int. Ed.*, 1989, **28**, 754-755.
23. A. Havlík, M. Lamač, J. Pinkas, Z. Padělková, A. Růžička, R. Gyepes and M. Horáček, *J. Organomet. Chem.*, 2012, **719**, 64-73.

24. A. Havlík, M. Lamač, J. Pinkas, V. Varga, A. Růžička, R. Olejník and M. Horáček, *J. Organomet. Chem.*, 2015, **786**, 71-80.
25. H. J. Reich, 2002.
26. a) H. Lang, R. Packheiser and B. Walfort, *Organometallics*, 2006, **25**, 1836-1850; b) R. Packheiser, P. Ecorchard, T. Ruffer and H. Lang, *Organometallics*, 2008, **27**, 3534-3546; c) R. Packheiser, A. Jakob, P. Ecorchard, B. Walfort and H. Lang, *Organometallics*, 2008, **27**, 1214-1226.
27. a) P. Pyykko and M. Atsumi, *Chem. Eur. J.*, 2009, **15**, 186-197; b) P. Pyykko and M. Atsumi, *Chem. Eur. J.*, 2009, **15**, 12770-12779; c) P. Pyykko, S. Riedel and M. Patzschke, *Chem. Eur. J.*, 2005, **11**, 3511-3520.
28. a) J. Bareš, P. Richard, P. Meunier, N. Pirio, Z. Padělková, Z. Černošek, I. Císařová and A. Růžička, *Organometallics*, 2009, **28**, 3105-3108; b) Z. Padělková, A. Havlík, P. Švec, M. S. Nechaev and A. Růžička, *J. Organomet. Chem.*, 2010, **695**, 2651-2657.
29. a) J. Bareš, V. Sourek, Z. Padělková, P. Meunier, N. Pirio, I. Císařová, A. Růžička and J. Holeček, *Collect. Czech. Chem. Commun.*, 2010, **75**, 121-131; b) H. Vaňkátová, L. Broeckart, F. De Proft, R. Olejník, J. Turek, Z. Padělková and A. Růžička, *Inorg. Chem.*, 2011, **50**, 9454-9464.
30. Z. Otwinowski and W. Minor, *Method Enzymol*, 1997, **276**, 307-326.
31. C. P., *Crystallographic Computing*, Munksgaard, Copenhagen, 1970.
32. A. Altomare, G. Cascarano, C. Giacovazzo and A. Guagliardi, *J Appl Crystallogr*, 1993, **26**, 343-350.
33. G. M. Sheldrick and T. R. Schneider, *Method Enzymol*, 1997, **277**, 319-343.
34. P. Vandersluis and A. L. Spek, *Acta Crystallogr A*, 1990, **46**, 194-201.